Forced Rossby Waves in a Zero Absolute Vorticity Gradient Environment

Paul F. Choboter
Department of Mathematics and Statistics
McGill University, Montreal

July, 1997

A thesis submitted to the Faculty of Graduate Studies and Research
in partial fulfilment of the requirements of the degree of
Master of Science

Abstract

Observations show the presence of localized regions in the atmosphere with diminished potential vorticity gradients, like in the tropical upper troposphere where outflow from deep convective regions plays an important role. The present work investigates the effect of forcing on the evolution of Rossby waves in a zero potential vorticity gradient environment. As a preliminary investigation, the barotropic case is studied, where the analogue of potential vorticity is absolute vorticity.

The analytic solution of the linearized problem shows that the streamfunction grows algebraically in time, and eventually develops a nonlinear critical layer. The numerical solution of the nonlinear problem within the critical layer shows that the nonlinearity and the forcing act together to halt the growth as coherent vortices are put in a nonlinear oscillatory regime. At long times, the critical layer solution settles to a quasi-steady state consisting of relatively large amplitude stationary vortices, with a set of small amplitude steadily-propagating vortices superimposed. These results are contrasted with the results of previous unforced problems.

Résumé

Les observations, par exemple dans la haute troposphère tropicale, nous montrent que l'atmosphère dans certaines régions a des gradients faibles de tourbillon potentiel. Nous avons étudié dans ce travail les effets de chauffage sur des perturbations cisaillées dans un environnement avec des gradients de tourbillon potentiel négligeables.

Nous concluons que dans l'approximation d'une perturbation infiniment petite, la fonction courant croît algébriquement dans la limite asymptotique et qu'une couche critique non linéaire se forme sous certaines conditions. La modélisation numérique de cette couche critique non linéaire montre que cette croissance algébrique est éventuellement stoppée et que nous obtenons l'établissement d'un régime oscillatoire non linéaire après une évolution complexe et transitoire. Ce régime oscillatoire consiste en une circulation stationnaire forcée sur laquelle est superposée une onde de Rossby discrète. Ces résultats sont contrastés avec les résultats de problèmes non forcées antérieures.

Acknowledgements

I would like to express my thanks to my thesis supervisor Professor Sherwin Maslowe for all his help in the research for and the writing of this thesis. Thank you also to Dr. Gilbert Brunet of Environment Canada for originally proposing the project and for making frequent trips to McGill to field my questions. Thanks as well to Professor Tom Warn for some helpful comments.

I gratefully acknowledge the financial support provided by the Natural Sciences and Engineering Research Council in the form of their Postgraduate Scholarship.

Finally, words cannot begin to express my appreciation for my wife, Denise, without whose encouragement and support this thesis would not have been possible.

Contents

List of Figures

Chapter 1

Introduction

In the theory of hydrodynamic stability of a parallel flow, the equations of motion are linearized by assuming the fluid velocities can be written as small perturbations to a known shear flow, $(u, v) = (U(y), 0)$, where u and v represent the velocities in the x and y directions respectively. For nondivergent flow, i.e. where $\nabla \cdot \mathbf{v} = 0$ (which is true in two dimensional flow where the variation of density is neglected), the velocity is specified by the streamfunction, ψ, via the relations

$$\frac{\partial \psi}{\partial x} = v \quad , \quad \frac{\partial \psi}{\partial y} = -u.$$

Typically, the streamfunction is assumed to be sinusoidal in the x direction, with a given wavenumber and phase speed. The flow is said to encounter a *critical level* at that value of y where the phase speed equals the speed of the shear flow. Here, the solution possesses a singularity. To circumvent this difficulty, some previously neglected process (such as nonlinearity, viscosity, or time dependence) is reintroduced

in a thin region about the critical level, called the *critical layer.* (See Maslowe 1986 for a complete discussion of critical layers.)

The barotropic vorticity equation is often used in simplified studies as the equation governing large-scale flows in the atmosphere. We will refer to any planetary-scale wave which solves this equation as a *Rossby wave.* (Strictly speaking, this definition is not quite complete. See below.) The linearized form of this equation, with primes denoting perturbation quantities, is

$$\frac{\partial \zeta'}{\partial t} + U(y)\frac{\partial \zeta'}{\partial x} + \left(\beta - \frac{d^2U}{dy^2}\right)\frac{\partial \psi'}{\partial x} = 0, \tag{1.1}$$

where the x direction is eastward, the y direction is northward, ζ is the relative vorticity, and β is the gradient of the planetary vorticity, assumed constant. The relative vorticity is the vertical component of the vorticity arising from the motion of the fluid: $\zeta = \mathbf{k} \cdot \nabla \times \mathbf{v}$, and therefore $\zeta = \nabla^2\psi$. The planetary vorticity, f, is the vertical component of the vorticity due to the rotation of the Earth. The parameter β is defined in the *beta plane approximation*, where a locally valid approximation to f is written $f \approx f_0 + \beta y$, with f_0 and β being constants which depend only on the latitude about which the approximation is made. Since this study is intended to apply to the tropical regions, it should be noted that the beta plane approximation is as valid in the tropics as in the midlatitudes. However, the assumption that $\beta y \ll f_0$ (which is made, for example, in quasi-geostrophic theory) is not valid in the tropics, since f decreases to zero at the equator (Holton 1992 §6.2). Such an assumption is not employed in this study, so the beta plane approximation is used with confidence.

The barotropic vorticity equation, in its fully nonlinear form, is a statement of the conservation of absolute vorticity, $\zeta+f$. Note that $\beta-U''$ is the leading-order gradient of absolute vorticity. The absolute vorticity gradient plays an important role in the propagation of Rossby waves, since it provides the restoring force necessary for the wave to propagate. It is readily seen from equation (1.1) above that if the absolute vorticity gradient were to vanish in a region, then the linear solution would be that of sheared disturbances. That is, the disturbance vorticity would simply be propagated in the x direction along lines of constant y at the phase speed $U(y)$. The solution at any given y value is not affected by the solution at any other value of y. That is why the solution is only a true Rossby wave if the absolute vorticity gradient is not identically zero in a region. In this thesis, when the leading-order gradient of absolute vorticity is zero, we will still refer to the solution as a Rossby wave because, as we will see, nonlinear effects allow the solution to depart from the sheared disturbance form.

Given that the vanishing of the absolute vorticity gradient yields a very particular motion, one may say that the problem is interesting from a mathematical point of view. However, can one say that it is a truly relevant problem? Do observations tell us that the leading order gradient of absolute vorticity is negligible in regions of the atmosphere? In fact, the answer is yes, particularly within the framework of isentropic coordinates and potential vorticity, in certain regions of the troposphere (Hoskins 1991 and Edouard *et al.* 1997. See below).

In isentropic coordinates, the potential temperature, θ, is used in the governing equations of the atmosphere as the vertical coordinate. In physical terms, the potential temperature is the temperature that a given parcel of dry air would have if it were brought adiabatically to sea level (Holton 1992). Over large planetary scales and at high enough distances above the ground, the potential temperature is observed to be a monotonic function of height, so it may be used as the vertical coordinate. The isentropic potential vorticity, hereafter PV (but denoted in equations as P), after using the hydrostatic approximation, is given by

$$P = \frac{\zeta_\theta + f}{\sigma},$$

where

$$\sigma = -\frac{1}{g}\frac{\partial p}{\partial \theta}$$

is the the density (or layer thickness) in isentropic coordinates, and ζ_θ is the relative vorticity evaluated on a constant-θ surface. Neglecting "tilting" and friction effects, the governing equation for PV is (Hoskins *et al.* 1985)

$$\frac{\partial P}{\partial t} + \mathbf{v} \cdot \nabla P = -\dot{\theta}\frac{\partial P}{\partial \theta} + P\frac{\partial \dot{\theta}}{\partial \theta}, \tag{1.2}$$

where $\dot{\theta}$ denotes $d\theta/dt$, the diabatic heating rate. Thus, the equation for PV in the absence of heating is simply the statement that it is materially conserved on constant-θ surfaces. The distinguishing characteristics of the PV framework include (1) the fact that PV acts like a physical tracer on constant-θ surfaces in the atmosphere, and (2) the existence of the "invertibility principle" of isentropic coordinates (Hoskins

et al. 1985).

It has been observed that PV gradients are small in some regions of the troposphere, like in the tropics. Hoskins (1991) reports of observational data which show that PV is nearly constant in a region about the equator, particularly so in regions of outflow from deep convective regions. Edouard *et al.* (1997), in their detailed study of the distribution of PV in the atmosphere, also find that PV gradients are small in the tropical upper troposphere. A mechanism by which PV gradients are diminished is eddy stirring of PV in the atmosphere, as seen for example in the numerical experiments of Juckes and McIntyre (1987; see also Brunet *et al.* 1995).

Note that PV is a three-dimensional quantity, but the two-dimensional analogue of PV is indeed absolute vorticity. Specifically, to claim that observed diminished PV gradients motivates a barotropic study with the gradient of absolute vorticity neglected, which is what we propose to do, is to perform that study on a constant-θ surface and to assume the isentropic density is constant.

The $\beta - U'' = 0$ case has been studied previously. Brunet and Warn (1990) studied the problem where the shear flow was taken to be $U(y) = \frac{\beta}{2}y^2$ as an example of a free, linear initial value problem with smooth initial conditions which developed a nonlinear critical layer in a finite time. (In the free, linear problem where the background shear flow has a linear profile, Tung (1983) proved that the problem would remain linear for all time.) They studied the linear problem and derived the leading-order nonlinear critical layer equations. Brunet and Haynes (1995) extended the solution to the case

where $\beta - U''$ is small but nonzero, and numerically studied the evolution of the nonlinear critical layer. The present study is closely related to this latter work, and much of the notation herein was chosen to be consistent with it.

Lindzen (1994) has also studied the zero PV gradient problem, but from a slightly different approach. He takes the normal mode approach to the three-dimensional problem, taking the shear flow to be linear in y and z and adjusting the Brunt-Väisälä frequency to set the PV gradient to zero.

In the framework of isentropic coordinates, vertical gradients of heating in the atmosphere act as PV sources and sinks, as can be seen from equation (1.2) (see also Hoskins 1991 and Hoerling 1992). Edouard *et al.* (1997) observed strong PV forcing near and above the tropopause. There, the tops of clouds provide the required variation of heating with height necessary to act as PV sources. They also found specific areas within the troposphere, located over the tropical Atlantic and Pacific oceans (see Figure 5b of Edouard *et al.* 1997), which are significant sources and sinks of PV. These areas are of relevance to this study because they coincide with areas of diminished PV gradients (see Figure 3b of Edouard *et al.* 1997).

One must be careful when one speaks of a "source" of PV. Haynes and McIntyre (1987) proved that PV cannot be transported through an isentropic surface, and that PV cannot be created nor destroyed in a region between two isentropic surfaces. However, PV may be created or destroyed at the edge of an isentropic surface (where it intersects the ground, for example), it may be transported along a constant-θ surface,

and it may be concentrated or diluted by the bounding isentropic surfaces squeezing together or spreading apart. Therefore, when we specify a source of PV, we in fact specify an effective source where PV is merely concentrated as isentropic surfaces come together.

A well-studied forced Rossby wave problem is the one in which the shear flow is linear and the Rossby wave is forced, usually by a corrugated wall, at the northern boundary. The Rossby wave propagates southward until it encounters a critical level (e.g. Stewartson 1978; Warn and Warn 1978; Killworth and McIntyre 1985; Ritchie 1985; Brunet and Haynes 1996, and further references therein). The presence of the critical layer profoundly affects the flow, first absorbing then reflecting the wave.

For example, Brunet and Haynes (1996) study the case where the forcing is localized in the x direction. They performed numerical simulations of the shallow-water model with the forcing in the form of ground topography, and found that, for a large enough forcing amplitude, the southward-propagating wave encounters a nonlinear wave-breaking region at the critical layer. The nonlinear wave activity, in turn, acts as a wave source to generate a "reflected" wave which indeed propagates northward, and not eastward along the critical layer.

In a study of a forced Rossby wave problem with a zero absolute vorticity gradient, however, the forcing must necessarily be in the form of a source term, as opposed to boundary condition forcing. Since the lack of communication between y levels means the Rossby wave cannot propagate, the problem with boundary forcing would not

make sense. Additionally, as seen above, the physics of a Rossby wave as forced by diabatic heating may be properly modeled by the addition of a source term. However, since the Rossby wave cannot propagate away from the source, one may expect a perpetual build-up of vorticity near the source, which is certainly not realistic behaviour. For example, in the unforced problem, the streamfunction in the finite PV gradient case decays as t^{-2} (Brown and Stewartson 1980), but in the zero gradient case the decay is only as $t^{-\frac{1}{2}}$ (except in the nonlinear critical layer, where the decay is halted; see Brunet and Haynes 1995). Therefore, a study of the forced problem would be interesting in the sense that it would answer the question of whether or not an unbounded increase of the streamfunction or the relative vorticity is the result of such a model.

The present work investigates the evolution of a forced Rossby wave in a zero absolute vorticity gradient environment. Initially, the perturbations to the basic state will be taken to be small so that the linearized problem may be studied, and the evolution of the initial-value problem will be sought. It will be seen that concepts from hydrodynamic stability, such as the presence of a nonlinear critical layer, will be relevant here even though no single phase speed is chosen for the solution.

The thesis is organized as follows. In chapter 2, the governing equations will be presented, and the solution to the linearized problem will be discussed. In chapter 3, the method of matched asymptotic expansions will be employed to find the leading-order equations at timescales on which the nonlinear terms may not be neglected.

The numerical methods used to solve the nonlinear equations are described in chapter 4. In chapter 5, the results of the numerical investigation are presented, and the concluding discussion of the results may be found in chapter 6. Appendix A presents the asymptotic analysis of the solution to the linearized problem with an alternate form of the forcing. That form of the forcing was ultimately not investigated numerically because the importance of the nonlinear terms was not confined to a critical layer.

Chapter 2

The Linearized Problem

2.1 The Governing Equations

Restricting our study to the evolution of vorticity on a given isentropic surface, we study the two-dimensional problem. The forcing will be modeled by a function to be specified which does not depend on the vorticity. Thus, the starting point for this investigation is the barotropic vorticity equation on a beta plane with a forcing term on the right hand side,

$$\frac{\partial \hat{\zeta}}{\partial t} - \frac{\partial \Psi}{\partial y}\frac{\partial \hat{\zeta}}{\partial x} + \frac{\partial \Psi}{\partial x}\frac{\partial \hat{\zeta}}{\partial y} + \beta\frac{\partial \Psi}{\partial x} = \epsilon S(x, y, t) \tag{2.1}$$

where $\epsilon \ll 1$, Ψ is the total (leading order plus $O(\epsilon)$ perturbation) streamfunction and $\hat{\zeta}$ is the total relative vorticity, so that $\nabla^2\Psi = \hat{\zeta}$. The horizontal derivatives are to be taken along an isentropic surface. By writing the forcing as ϵS, we are assuming that it comes into play at the order of the disturbances to the shear flow. The equation is

linearized about a shear flow $u = U(y)$ by writing

$$\Psi = -\int^y U(y')\,dy' + \epsilon\psi \quad \text{and} \quad \hat{\zeta} = -\frac{dU}{dy} + \epsilon\zeta \tag{2.2}$$

so that, assuming that the shear flow itself solves the leading-order equation, the governing equation becomes

$$\frac{\partial\zeta}{\partial t} + U(y)\frac{\partial\zeta}{\partial x} + (\beta - U'')\frac{\partial\psi}{\partial x} + \epsilon\left(\frac{\partial\psi}{\partial x}\frac{\partial\zeta}{\partial y} - \frac{\partial\psi}{\partial y}\frac{\partial\zeta}{\partial x}\right) = S(x,y,t). \tag{2.3}$$

Wishing to study the dynamics of a region where the absolute vorticity gradient is weak, we set $\beta - U'' = 0$ by choosing $U(y) = U_0 + \frac{\beta}{2}y^2$, where U_0 is constant and represents the constant (unsheared) part of the background flow. U_0 may be removed from the left side of equation (2.3) by making a Galilean transformation of coordinates: $(x, y, t) \to (x - U_0 t, y, t)$. The linearized problem is then

$$\frac{\partial\zeta}{\partial t} + \frac{\beta}{2}y^2\frac{\partial\zeta}{\partial x} = S(x + U_0 t, y, t), \tag{2.4}$$

which, by the method of characteristics, has the formal solution

$$\zeta(x,y,t) = \zeta_0\left(x - \tfrac{\beta}{2}y^2 t, y\right) + \int_0^t S\left(x - \tfrac{\beta}{2}y^2(t-t') + U_0 t', y, t'\right)\,dt', \tag{2.5}$$

where $\zeta_0(x,y) = \zeta(x,y,0)$ is the arbitrary initial condition. The solution for ψ is found via $\nabla^2\psi = \zeta$, along with the boundary conditions which require that ψ remain bounded as x or $y \to \pm\infty$.

2.2 The Stationary Forcing Problem

In order to be able to evaluate the integral in (2.5), a specific form of the forcing function is chosen. We choose to model the forcing by a function which is periodic in x, is of an undetermined form in y, and travels in the x direction with the same (constant) speed as the unsheared part of the background flow, U_0;

$$S(x, y, t) = \sigma(y) e^{ik(x - U_0 t)}. \tag{2.6}$$

(Throughout the theoretical part of this investigation, it is to be understood that complex functions such as S, and later, the solutions for ζ and ψ, stand for their real parts.) This form of the forcing is independent of time in the frame of reference moving with speed U_0. Thus, with respect to the sheared part of the background flow, it is stationary. This forcing has been chosen for its simplicity, and, unfortunately, is somewhat artificial. A more general form of the forcing, one which travels even in this frame of reference, has also been investigated, with the details provided in Appendix A. (See Chapter 6: Conclusions for a discussion of which forcing functions would be more realistic.)

The stationary forcing case might best be thought of as modeling the PV forcing in the region over the tropical Atlantic. There, the observed background wind flow is weak (Grotjahn 1993, Figure 5.7).

With the above forcing, the solution for the vorticity, equation (2.5), then becomes

$$\zeta(x, y, t) = \zeta_0 \left(x - \tfrac{\beta}{2} y^2 t, y \right) + \sigma(y) \frac{\sin\left(\frac{k\beta}{4} y^2 t\right)}{\frac{k\beta}{4} y^2} e^{ik\left(x - \frac{\beta}{4} y^2 t\right)}. \tag{2.7}$$

Note that the second term is actually a difference of two complex exponential terms. It is written in terms of the sine function (using the complex definition of $\sin x$) to make it easy to see that there is *not* a singularity at $y = 0$.

It merely remains to invert Poisson's equation and solve for ψ. Notice that ζ has one term arising from the forcing and another term corresponding to the unforced problem that was studied by Brunet and Warn (1990, hereafter referred to as BW). Assuming the solution is periodic in x, we write $\zeta_0 = \Omega_0(y)e^{ikx}$ and $\psi = e^{ikx}\Phi(y,t)$. (Implicitly, we have also assumed here that the initial condition has the same wavenumber as the forcing, which, strictly speaking, is not necessarily true. However, the making of this assumption does not affect the results. It is made merely to simplify the notation.) Then Poisson's equation in ψ becomes an inhomogeneous O.D.E. in Φ, which, by the method of Green's functions, has the following solution:

$$\begin{aligned}\Phi(y,t) &= -\frac{1}{2k}\int_{-\infty}^{\infty} e^{-k|y-\xi|}\Omega_0(\xi)e^{-i\frac{k\beta}{2}\xi^2 t}\,d\xi \\ &\quad -\frac{1}{2k}\int_{-\infty}^{\infty} \sigma(\xi)\frac{\sin\left(\frac{k\beta}{4}\xi^2 t\right)}{\frac{k\beta}{4}\xi^2}e^{-k|y-\xi|}e^{-i\frac{k\beta}{4}\xi^2 t}\,d\xi \\ &= \Phi_1 + \Phi_2, \end{aligned} \tag{2.8}$$

where Φ_1 is exactly the result that was arrived at in BW, and Φ_2 is the new term arising as a result of the forcing. When $y = O(1)$, the behaviour of Φ_1 for large values of t, as found by BW, is

$$\Phi_1 \sim -\left(\frac{\pi}{2k\beta t}\right)^{1/2}\Omega_0(0)\frac{e^{-i\pi/4}}{k}e^{-k|y|} + O(t^{-1}). \tag{2.9}$$

To determine the long-time asymptotic nature of Φ_2, the integral is written in two

parts to eliminate the absolute value signs,

$$\Phi_2 = -\frac{1}{2k}\left[\int_{-\infty}^{y}\sigma(\xi)\frac{\sin\left(\frac{k\beta}{4}\xi^2 t\right)}{\frac{k\beta}{4}\xi^2}e^{-k(y-\xi)}e^{-i\frac{k\beta}{4}\xi^2 t}\,d\xi + \int_{y}^{\infty}\sigma(\xi)\frac{\sin\left(\frac{k\beta}{4}\xi^2 t\right)}{\frac{k\beta}{4}\xi^2}e^{-k(\xi-y)}e^{-i\frac{k\beta}{4}\xi^2 t}\,d\xi\right]. \tag{2.10}$$

From this form, notice that if $y = O(1)$ then the asymptotic behaviour of Φ_2 may be found by the method of stationary phase, since the stationary phase point at $\xi = 0$ will be well within only one of the two integrals. However, if $y = O(t^{-1/2})$, then the stationary phase point is not well separated from the y endpoints of the integrals, so the contributions from both integrals at the same time must be evaluated. In this respect, separate investigations of an outer region and an inner region are to be conducted.

2.3 The Outer Solution

If $y = O(1)$, then for $y > 0$, the first of the two integrals in equation (2.10) will contain the $\xi = 0$ stationary phase point. Since the greatest contribution to the integral will be near $\xi = 0$ the approximation $\sigma(\xi)e^{-k(y-\xi)} \approx \sigma(0)e^{-ky}$ may be made, so that

$$\Phi_2 \approx -\frac{\sigma(0)}{2k}e^{-ky}\int_{-\infty}^{y}\frac{\sin\left(\frac{k\beta}{4}\xi^2 t\right)}{\frac{k\beta}{4}\xi^2}e^{-i\frac{k\beta}{4}\xi^2 t}\,d\xi. \tag{2.11}$$

With the change of variables $s = \sqrt{\frac{k\beta t}{4}}\xi$, this becomes

$$\Phi_2 \sim -\frac{\sigma(0)}{k}\sqrt{\frac{t}{k\beta}}e^{-ky}\int_{-\infty}^{\infty}\frac{\sin(s^2)}{s^2}e^{-is^2}\,ds, \tag{2.12}$$

where the integral is merely an $O(1)$ complex constant. For $y < 0$, the analysis is identical to the $y < 0$ case, except that it is the other integral that contains the stationary phase point, so the result possesses the term e^{+ky} instead of e^{-ky}. Therefore, it is true for both cases that the large-t asymptotic behaviour for ψ when $y = O(1)$ is

$$\psi \sim -e^{ikx}\sqrt{\frac{t}{k\beta}}e^{-k|y|}\frac{2\sigma(0)}{k}\left[\int_{-\infty}^{\infty}\frac{\sin(s^2)}{s^2}e^{-is^2}\,ds\right]. \tag{2.13}$$

The fact that a separate analysis is required for the inner region is further indicated by the discontinuous y-derivative at $y = 0$.

The above asymptotic form for ψ, and equation (2.7) for ζ, may be used to determine the timescale at which the nonlinear terms of equation (2.3) take on leading-order importance in the outer region. Each term in the governing equation is of the indicated order, where subscripts denote partial derivatives:

$$\begin{array}{ccccccccc} \zeta_t & + & \frac{\beta}{2}y^2\zeta_x & + & \epsilon(\psi_x\zeta_y & - & \psi_y\zeta_x) & = & \sigma(y)e^{ikx} \\ O(1) & & O(1)O(1) & & \epsilon O(t^{1/2})O(t) & & \epsilon O(t^{1/2})O(1) & & O(1) \end{array}$$

so the nonlinear terms become important at $t = O(\epsilon^{-2/3})$.

2.4 The Inner Region Asymptotic Behaviour

The inner region is investigated by letting $\eta = \frac{1}{2}(k\beta t)^{1/2}y = O(1)$. Also, we denote equation (2.8) as $\Phi(\eta, t) = \tilde{\Phi}_1(\eta, t) + \tilde{\Phi}_2(\eta, t)$, so that $\tilde{\Phi}_1$ is the contribution from the

initial conditions and $\tilde{\Phi}_2$ is the contribution from the forcing. BW found that

$$\tilde{\Phi}_1 \sim \left[-\left(\frac{\pi}{2k\beta t}\right)^{1/2}\frac{e^{-i\pi/4}}{k} + \frac{2\sqrt{2}\eta}{k\beta t}\int_0^{\sqrt{2}\eta} e^{-is^2}\,ds\right]\Omega_0(0) + O(t^{-3/2}). \tag{2.14}$$

If the change of variables $s = \frac{1}{2}(k\beta t)^{1/2}\xi$ is made in the integrals of equation (2.10) then

$$\begin{aligned}\tilde{\Phi}_2 \;=\; -\frac{1}{k}\left(\frac{t}{k\beta}\right)^{1/2}\Bigg[&\int_{-\infty}^{\eta}\sigma\left(\frac{2s}{\sqrt{k\beta t}}\right)\frac{\sin(s^2)}{s^2}e^{-(\frac{4k}{\beta t})^{1/2}(\eta-s)}e^{-is^2}\,ds \\ &+\int_{\eta}^{\infty}\sigma\left(\frac{2s}{\sqrt{k\beta t}}\right)\frac{\sin(s^2)}{s^2}e^{-(\frac{4k}{\beta t})^{1/2}(s-\eta)}e^{-is^2}\,ds\Bigg].\end{aligned} \tag{2.15}$$

Assuming the integrand makes a negligible contribution to the integral when $s = O(t^{1/2})$ or larger (due to the integrand's oscillation in s and s^{-2} decay), the approximation $\sigma((k\beta t)^{-1/2}s) \approx \sigma(0)$ is employed. The integral then may be written in the form

$$\begin{aligned}\tilde{\Phi}_2 \;=\; -\frac{\sigma(0)}{k}\left(\frac{t}{k\beta}\right)^{1/2}\Bigg[&2\cosh\left(\left(\tfrac{4k}{\beta t}\right)^{1/2}\eta\right)\int_0^{\infty}\frac{\sin(s^2)}{s^2}e^{-(\frac{4k}{\beta t})^{1/2}s}e^{-is^2}\,ds \\ &+\int_0^{\eta} 2\sinh\left(\left(\tfrac{4k}{\beta t}\right)^{1/2}(s-\eta)\right)\frac{\sin(s^2)}{s^2}e^{-is^2}\,ds\Bigg].\end{aligned} \tag{2.16}$$

Finally, by expanding this expression in powers of t, it is found that

$$\begin{aligned}\tilde{\Phi}_2 \;\sim\; &-\frac{2\sigma(0)}{k}\left(\frac{t}{k\beta}\right)^{1/2}\int_0^{\infty}\frac{\sin(s^2)}{s^2}e^{-is^2}\,ds \\ &+\;\frac{4\sigma(0)}{k\beta}\left(\int_{\eta}^{\infty}\frac{\sin(s^2)}{s^2}e^{-is^2}\,ds + \eta\int_0^{\eta}\frac{\sin(s^2)}{s^2}e^{-is^2}\,ds\right) + O(t^{-1/2}).\end{aligned} \tag{2.17}$$

Thus, to leading order, $\psi \sim e^{ikx}\tilde{\Phi}_2$ since $\tilde{\Phi}_1 = O(t^{-1/2})$.

As was done for the outer region, the above asymptotic form and equation (2.7) are substituted into equation (2.3) to determine the order of magnitude of each term,

with the following result:

$$\begin{array}{ccccccc} \zeta_t & + & \frac{\beta}{2}y^2\zeta_x & + & \epsilon(\psi_x\zeta_y & - & \psi_y\zeta_x) & = & \sigma(y)e^{ikx} \\ O(1) & & O(t^{-1})O(t) & & \epsilon O(t^{1/2})O(t^{3/2}) & & \epsilon O(t^{1/2})O(t) & & O(1). \end{array}$$

Thus, the nonlinear terms become important in the critical layer when $t = O(\epsilon^{-1/2})$, which is before the outer region becomes nonlinear. Therefore, when $t = O(\epsilon^{-1/2})$, there exists a nonlinear critical layer region with the outer region solution remaining linear.

Chapter 3

The Nonlinear Regime

3.1 The Outer Region

According to the analysis of the previous chapter, the nonlinear regime is when $t = \epsilon^{-1/2}T$, where $T = O(1)$. The asymptotic forms found for the linear regime outer region, given by equations (2.13) and (2.7), suggest expansions (2.2) be replaced by

$$\Psi = -\tfrac{\beta}{6}y^3 + \epsilon^{3/4}\psi_{o\pm}^{(3/4)} + \epsilon\psi_{o\pm}^{(1)} \quad \text{and} \quad \hat{\zeta} = -\beta y + \epsilon\zeta_{o\pm}\,, \tag{3.1}$$

where the subscripts denote the outer region either above or below the critical layer. The relation between Ψ and $\hat{\zeta}$ yields, to leading order

$$\nabla^2\psi_{o\pm}^{(3/4)} = 0 \tag{3.2}$$

which is a result that will be referred to later in the analysis.

In anticipation of requiring a matching condition for the critical layer solution, we write the outer region expansion in terms of the inner variable, $Y = \epsilon^{-1/4}y$ through

a Taylor expansion in y

$$(\psi_o)_i = \epsilon^{3/4}\left[-\frac{\beta}{6}Y^3 + \psi_{o\pm}^{(3/4)}(x,0,T)\right] + \epsilon\left[Y\frac{\partial\psi_{o\pm}^{(3/4)}}{\partial y}(x,0,T) + \psi_{o\pm}^{(1)}(x,0,T)\right] + O(\epsilon^{5/4}). \tag{3.3}$$

3.2 The Nonlinear Critical Layer Region

The nonlinear critical layer is investigated by scaling the independent variables like $t = \epsilon^{-1/2}T$ and $y = \epsilon^{1/4}Y$, where T and Y are $O(1)$. The dependent variables have the following scaling, as suggested by the linear regime's inner region solution (given by (2.7) and (2.17)):

$$\Psi = \epsilon^{3/4}\psi_i^{(3/4)} + \epsilon\psi_i^{(1)} \quad \text{and} \quad \hat{\zeta} = \epsilon^{1/4}\zeta_i^{(1/4)} + \epsilon^{1/2}\zeta_i^{(1/2)}. \tag{3.4}$$

Then the leading-order relation between the vorticity and the streamfunction is $\zeta_i^{(1/4)} = \psi_{iYY}^{(3/4)}$, where subscripts following i denote partial derivatives. When the above expansion is substituted into the governing equation (2.1), and the result written entirely in terms of the streamfunction, the leading order equation in the critical layer is

$$\psi_{iYYT}^{(3/4)} + \psi_{ix}^{(3/4)}\psi_{iYYY}^{(3/4)} - \psi_{iY}^{(3/4)}\psi_{ixYY}^{(3/4)} + \beta\psi_{ix}^{(3/4)} = 0. \tag{3.5}$$

The integral of this equation from $-Y$ to Y yields

$$\left[\psi_{iYT}^{(3/4)} + \psi_{ix}^{(3/4)}\psi_{iYY}^{(3/4)} - \psi_{iY}^{(3/4)}\psi_{ixY}^{(3/4)}\right]_{-Y}^{Y} + \int_{-Y}^{Y}\beta\psi_{ix}^{(3/4)}\,dY' = 0. \tag{3.6}$$

Then the matching condition implied by equation (3.3), that is

$$\psi_i^{(3/4)} \sim -\frac{\beta}{6}Y^3 + \psi_{o\pm}^{(3/4)}(x,0,T) \quad \text{as} \quad Y \to \pm\infty, \tag{3.7}$$

may be used to show that

$$\int_{-Y}^{Y} \frac{\partial \psi_i^{(3/4)}}{\partial x}\, dY' = |Y|\Big(\frac{\partial \psi_{o+}^{(3/4)}}{\partial x} + \frac{\partial \psi_{o-}^{(3/4)}}{\partial x}\Big) \quad \text{as} \quad Y \to \pm\infty. \tag{3.8}$$

This indicates that $\psi_{ix}^{(3/4)}$ is independent of Y; therefore, $\psi_{o+}^{(3/4)} = \psi_{o-}^{(3/4)}$. Denoting $C(x,T) = \psi_{o+}^{3/4} = \psi_{o-}^{3/4}$, we may write

$$\psi_i^{(3/4)} = -\frac{\beta}{6}Y^3 + C(x,T) \tag{3.9}$$

since both equation (3.5) and the matching condition are then satisfied. This also means that $\zeta_i^{(3/4)} = -\beta Y$. The form of C is found by proceeding to the next order equation in the critical layer. Denoting $\zeta_i^{(1/2)} = Z(x,Y,T)$, the equation can be written

$$\frac{\partial Z}{\partial T} + \frac{\beta}{2}Y^2\frac{\partial Z}{\partial x} + \frac{\partial C}{\partial x}\frac{\partial Z}{\partial Y} = \sigma(0)e^{ikx}. \tag{3.10}$$

Note that at this order, the forcing term does finally play a role. This is the governing nonlinear equation for the critical layer region which will have to be integrated numerically.

It still remains to directly relate Z and C. This is done by first observing that $\psi_{iYY}^{(1)} = Z$, from which we find that $\psi_{iY}^{(1)} = \int Z\, dY$. Next, the matching condition suggested by equation (3.3),

$$\psi_i^{(1)} \sim Y\frac{\partial \psi_{o\pm}^{(3/4)}}{\partial y}(x,0,T) + \psi_{o\pm}^{(1)}(x,0,T) \quad \text{as} \quad Y \to \pm\infty, \tag{3.11}$$

is used to obtain the following jump condition:

$$\left[\frac{\partial \psi_{o\pm}^{(3/4)}}{\partial y}\right]_{0-}^{0+} = \int_{-\infty}^{\infty} Z\, dY. \tag{3.12}$$

Since we already have $\nabla^2 \psi_{o\pm}^{(3/4)} = 0$ and $\psi_{o\pm}^{(3/4)} = C(x,T)$ on $y = 0$, then a result from Sneddon (1972 §3.21) yields

$$\frac{\partial \psi_{o\pm}^{(3/4)}}{\partial y}(x,0,T) = \mp \frac{1}{\pi} \mathcal{P} \int_{-\infty}^{\infty} \frac{C_x(u,T)}{(u-x)}\, du, \tag{3.13}$$

where $\mathcal{P}$ denotes the Cauchy principal value of the integral. The jump condition then becomes

$$-\frac{2}{\pi} \mathcal{P} \int_{-\infty}^{\infty} \frac{C_x(u,T)}{(u-x)}\, du = \int_{-\infty}^{\infty} Z(x,Y,T)\, dY. \tag{3.14}$$

Finally, upon taking the Fourier transform with respect to x of this relation, and using a result from Hilbert transform theory, (see Maslowe and Redekopp 1979, and also Sneddon 1972 §3-21) it is found that

$$\tilde{C}(\alpha,T) = -\frac{1}{2|\alpha|} \int_{-\infty}^{\infty} \tilde{Z}(\alpha,Y,T)\, dY, \tag{3.15}$$

where α is the wavenumber in the x direction and the tildes denote the Fourier transforms of the respective functions. This is the relation between C and Z that will be used in numerically solving equation (3.10).

Chapter 4

Numerical Methods

The numerical method used to solve the nonlinear critical layer equations may be briefly summarized as follows. The first step is to scale the independent and dependent variables in order to eliminate the three parameters in the equations. For the calculations, a pseudo-spectral method is used in the x direction, and finite differences are used in the Y direction and for the time variable T. The critical layer vorticity, Z, is calculated at time $T + \Delta T$ from the solution at time T using a semi-implicit method. The tests for accuracy of the method include comparison with the unforced results, as obtained by Brunet and Haynes (1995), and comparison with the linearized results, for which we have an analytic form.

Equation (3.10) has three independent parameters: β, k and σ. It is possible to eliminate them by nondimensionalizing the variables in the equation. Denoting the

dimensional variables and parameters as primed,

$$x' = Lx, \quad Y' = L\sigma^{\frac{1}{4}}Y, \quad \alpha' = \alpha/L, \quad T' = T/(\tfrac{1}{2}\beta L\sigma^{\frac{1}{2}}),$$

$$k' = k/L, \quad \sigma' = \tfrac{1}{4}\beta^2 L^2\sigma, \quad C' = \tfrac{1}{2}\beta L^3\sigma^{\frac{3}{4}}C, \quad Z' = \tfrac{1}{2}\beta L\sigma^{\frac{1}{2}}Z,$$

where L has been introduced as the length scale. We have the freedom in the scaling to choose $L = 1/k'$, so that L is actually defined by the spatial extent of the forcing. Then equation (3.10) becomes

$$\frac{\partial Z}{\partial T} + Y^2\frac{\partial Z}{\partial x} + \frac{\partial C}{\partial x}\frac{\partial Z}{\partial Y} = \cos x \tag{4.1}$$

so that the critical layer equation is identical to what it was before the scaling, except that β is replaced by 2, k is replaced by 1, and σ is replaced by 1 (and we have written e^{ix} explicitly as its real part, $\cos x$). Equation (3.15) is unchanged in appearance by the nondimensionalization.

Next, motivated by the fact that the boundary condition (equation (3.15)) is in terms of the Fourier transforms of C and Z, we let

$$Z(x, Y, T) = Re\left[\sum_{n=0}^{N} Z_n(Y, T)e^{inx}\right]$$

$$C(x, T) = Re\left[\sum_{n=0}^{N} C_n(T)e^{inx}\right],$$

where N is taken to be 32. Note that, although the above expressions *define* the relationship between Z_n and Z, the conversion between Fourier space and physical space is accomplished in practice using Fast Fourier Transforms (see Press *et al.* 1992). The physical space function is made real by projecting the $N + 1$ terms onto

an intermediate set of $2N$ terms with symmetries designed to exactly cancel the imaginary part, that is

$$Z_n^i = \begin{cases} Re(Z_n) & , n = 0 \text{ or } n = N \\ \frac{1}{2} Z_n & , n = 1, 2, \ldots, N-1 \\ \frac{1}{2} Z_{2N-n}^* & , n = N+1, \ldots, 2N-1 \end{cases} \tag{4.2}$$

where Z_n^i denotes the intermediate terms and the asterisk denotes complex conjugate. Applying the Fast Fourier Transform to Z_n^i then produces the real function Z. The transform process is performed in the same way for C.

The time stepping procedure evaluates the time derivative as in a forward difference scheme, and the shear flow advection term as in a trapezoidal scheme. Weak viscosity is introduced into the problem to remove unphysical gridscale structures; the magnitude of its effect is controlled through the parameter λ (see below for a discussion of how λ is chosen). Upon denoting the nonlinear term as P_n, equation (4.1) therefore becomes

$$\frac{Z_n^{T+\Delta T} - Z_n^T}{\Delta T} + \frac{1}{2} inY^2 \left(Z_n^{T+\Delta T} + Z_n^T \right) + P_n^{P\text{-}C} = \delta_{1n} + \lambda \frac{\partial^2 Z_n^T}{\partial Y^2}, \tag{4.3}$$

where the superscripts T and $T+\Delta T$ denote evaluation at the present time step and at the subsequent time step respectively, and P-C indicates that the predictor-corrector method is used. The shear flow, Y^2, is quite large near the edge of the computational domain; therefore, it would severely restrict the size of the time step that numerical stability would allow if the term it multiplies were evaluated explicitly. An advantage of using the above scheme to perform the time stepping is that the term multiplied by

the shear flow is evaluated semi-implicitly, but $Z_n^{T+\Delta T}$ may still be explicitly solved for, so the time stepping may proceed explicitly.

The nonlinear term, written above as P_n, is the nth Fourier mode of the term $(\partial Z/\partial Y)(\partial C/\partial x)$. It is calculated by the *pseudo-spectral* method. That is, instead of performing the convolution product directly in Fourier space, the functions are transformed into real space functions, multiplied in real space, and the function of the product is transformed back into Fourier space to produce P_n. This method of evaluating such a nonlinear term is known to be more efficient than directly evaluating the convolution product in Fourier space, as long as Fast Fourier Transforms are used.

Aliasing effects are removed from the calculation of P_n by padding the Fourier space modes with zeros. Specifically, this is done by projecting the intermediate mode onto a set of 4N terms, where the 2N terms that correspond to the highest wavenumbers are set to zero (see Press *et al.* 1992 §13.1, for a discussion of aliasing effects and their removal by zero padding).

With respect to the time stepping procedure, P_n is evaluated using a predictor-corrector method. First, a temporary value of $Z_n^{T+\Delta T}$ is calculated by using Z_n^T in the calculation of P_n. Then, the temporary value of $Z_n^{T+\Delta T}$ is used in the calculation of P_n as the actual $Z_n^{T+\Delta T}$ is calculated. This technique, as opposed to merely evaluating P_n once per time step using Z_n^T, was observed to significantly improve the numerical stability of the calculations.

The viscosity term is added to remove gridscale features which would otherwise

spontaneously appear in the solution, and eventually dominate the behaviour, but are not a result of the dynamics in which we are interested. The strength of the viscosity is controlled by the parameter λ, which was set to the smallest value that still resulted in the removal the gridscale features. For comparison with the unforced problem, a value of 0.01 was used. However, it turns out that, in the forced problem using $\lambda = 0.01$, the effect of the viscosity is seen in a particular aspect of the dynamics (see Chapter 5: Numerical Results, below). Therefore, λ was set to 0.001, a value at which the viscosity has no effect on the dynamics.

The Y-derivatives of equation (4.1) are evaluated by centered difference approximations. At the edges of the computational domain, the centered difference is replaced by the appropriate one-sided difference. For all the calculations reported here, the computational domain in the Y direction was $-7.5 \leq Y \leq 7.5$, with 151 grid points used (i.e. making $\Delta Y = 0.1$).

The initial condition was taken to be $Z(x, Y, 0) = 0$. One can see that this should be the case by substituting the critical layer variables ($y = \epsilon^{1/4} Y$ and $t = \epsilon^{-1/2} T$) into equation (2.7). Then the term resulting from the forcing, which is the leading order term and the one which matches to Z, is seen to go to zero as T goes to zero.

The critical layer streamfunction, C, is equal to an infinite integral of Z in the Y direction. However, Z is only known in the computational domain, taken here to be $-7.5 \leq Y \leq 7.5$. This was dealt with by assuming C to be approximately equal to

the integral of Z over the computational domain only:

$$C_n \approx -\frac{1}{2n}\int_{-7.5}^{7.5} Z_n \, dY.$$

The amount of error introduced by making this approximation may be estimated by assuming that, outside the computational domain, Z_n is equal to its value at linear times (given by equation (2.7)). Since the initial condition is zero, only Z_1 is nonzero in this approximation. The error in C_1 may then be written

$$\begin{aligned} \text{error} &= -\int_{7.5}^{\infty} \frac{\sin(\frac{1}{2}Y^2T)}{\frac{1}{2}Y^2} e^{-\frac{1}{2}iY^2T}\, dY \\ &= -\left(\frac{T}{2}\right)^{\frac{1}{2}} \int_{7.5\left(\frac{T}{2}\right)^{1/2}}^{\infty} \frac{\sin s^2}{s^2} e^{-is^2}\, ds. \end{aligned}$$

Numerical approximations of this expression show that for $T > 0$, it is constant in time, at approximately $-0.06i$. In an *a posteriori* evaluation, this value is less than 5% of the value of C_1 for most times (see Chapter 5: Numerical Results, below).

The time step was chosen to have various values for different calculations, but in general it was taken to be less than 0.0005. Higher values of ΔT led to numerical instability overtaking the solution. Note that this instability was seen even for values of ΔT where the *Courant-Friedrichs-Lewy* (CFL) criterion, which requires $\Delta T < \Delta x/U_{max}$ for convergence, was satisfied. For example, with $\Delta x \approx 0.1$ (since there are 63 waves when $N = 32$) and $U_{max} = 56.25$, the CFL criterion requires $\Delta T < 0.0018$, but the instability was still seen at $\Delta T = 0.001$. Figure (4.1) demonstrates the typical behaviour of the instability, which was seen as exponential growth in time, localized near a particular wavenumber, $n = n_i$, and particular Y values, $Y = \pm Y_i$.

a)

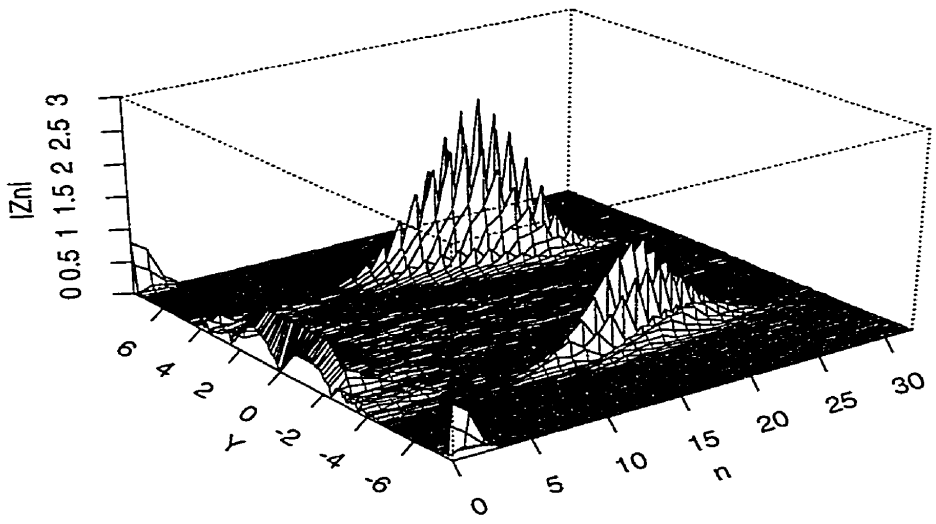

b)

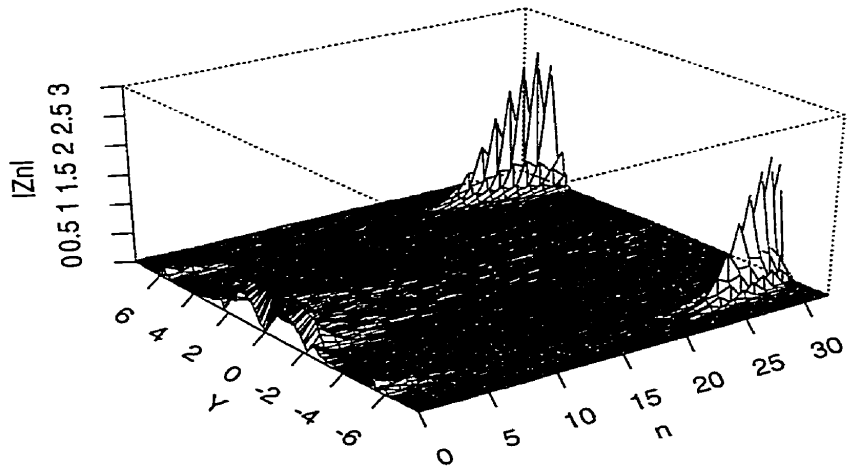

Figure 4.1: Numerical instability: Fourier space plots of $|Z_n|$ versus n and Y when instability occurs. In each case, $\lambda = 0.001$. (a): $\Delta T = 0.01$. $T = 7.43$ is shown. (b): $\Delta T = 0.001$. $T = 6.976$ is shown.

As ΔT is decreased, n_i and Y_i each increase. So by taking ΔT small enough, the instability was removed entirely from the domain of the problem. For most runs, choosing $\Delta T = 0.0002$ sufficed to eliminate the instability.

Chapter 5

Nonlinear Results

5.1 Comparison with Unforced Results

The results of the unforced problem are presented first, since any solution to the forced problem will be contrasted with these unforced results. Also, the ability of this numerical scheme to reproduce the previous results allows us to have confidence in the accuracy of the forced problem results.

Brunet and Warn (1990) found that the streamfunction of the linearized unforced problem decays like $\psi \sim t^{-1/2}$ and the vorticity consists of the initial condition, sheared in time with the parabolic flow. Brunet and Haynes (1995) found numerically that, in the nonlinear critical layer, the effect of the nonlinearity is to halt the decay of the streamfunction and to form coherent vortices which propagate in the x direction with a constant phase speed. These results have been reproduced, and are displayed

in figure (5.1). The significance of showing the sine and cosine components of C_1 is that the change in the relative sizes of these values corresponds to a phase change in the disturbance. So the behaviour seen in the nonlinear plot of C_1 indicates that the vorticity field settles toward a state where the vortices travel in the positive x direction with a steady speed.

The solution of the forced problem is shown in figure (5.2). The solution of the linearized problem is seen to agree with the asymptotic analysis which predicted $O(T^{1/2})$ growth in the amplitude of the streamfunction and growth in the vorticity which is strongest, i.e. $O(T)$, at $Y = 0$.

The nonlinearity affects the solution significantly. For example, the growth of the streamfuction is halted. In fact, its amplitude oscillates about a nonzero value with a fixed frequency and a decaying amplitude. The vorticity, while forming coherent structures similar to that seen in the unforced case, does not exhibit the same kind of translational motion as that solution, as will be shown below.

The decay in the streamfunction amplitude oscillation is *not* due to the viscosity added to the problem. The viscosity parameter, λ, was varied to obtain the least amplitude decay while still preventing the emergence of grid-scale structures, and it was found that the decay of the streamfunction amplitude oscillation is independent of λ when $\lambda < 0.001$. Indeed, the decay appears to be the same for $\lambda = 0$ as for $\lambda = 0.001$.

However, the amplitude of the oscillation does not decay to zero. (At least, not

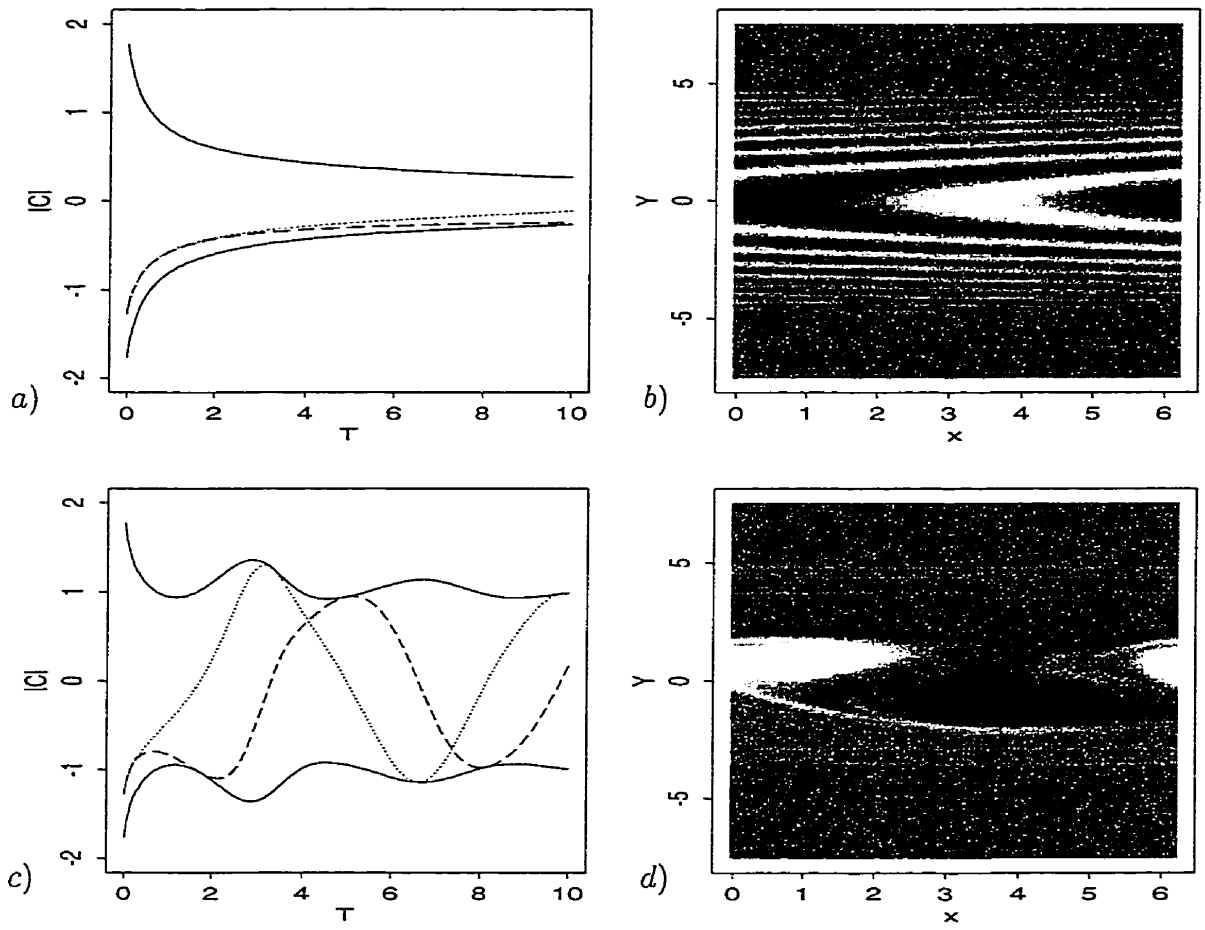

Figure 5.1: Linear and nonlinear unforced results. (a) and (c): First Fourier coefficient of C, linear and nonlinear cases. Dotted and dashed lines are the cosine and sine components, respectively. (b) and (d): Z in linear and nonlinear cases, at $T = 2$, $T = 4$. Greyscale: black=+1, white=-1.

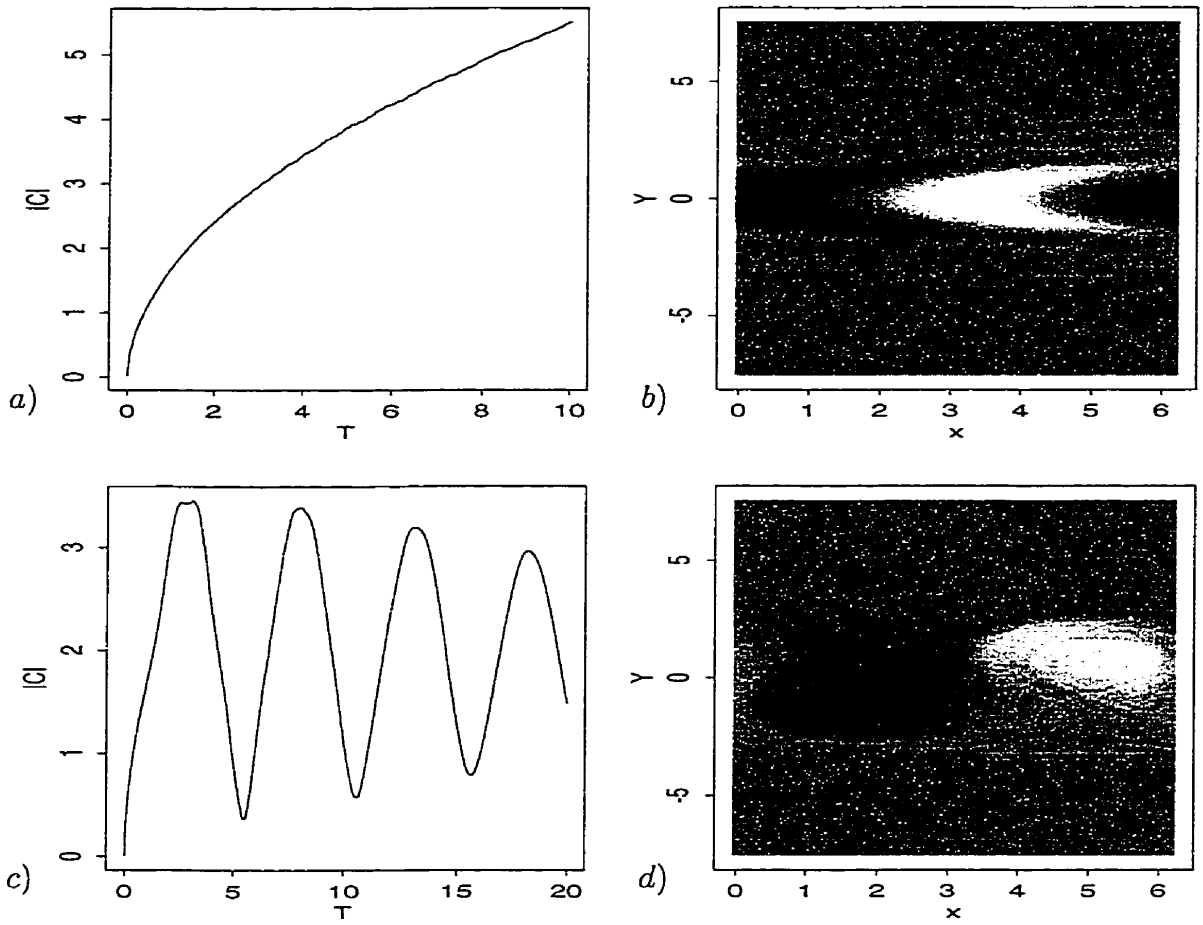

Figure 5.2: Linearized and nonlinear forced results. (a) and (c): First Fourier coefficient of C, linearized and nonlinear cases. (b) and (d): Z in linearized and nonlinear cases, at $T = 2$, $T = 3.2$.

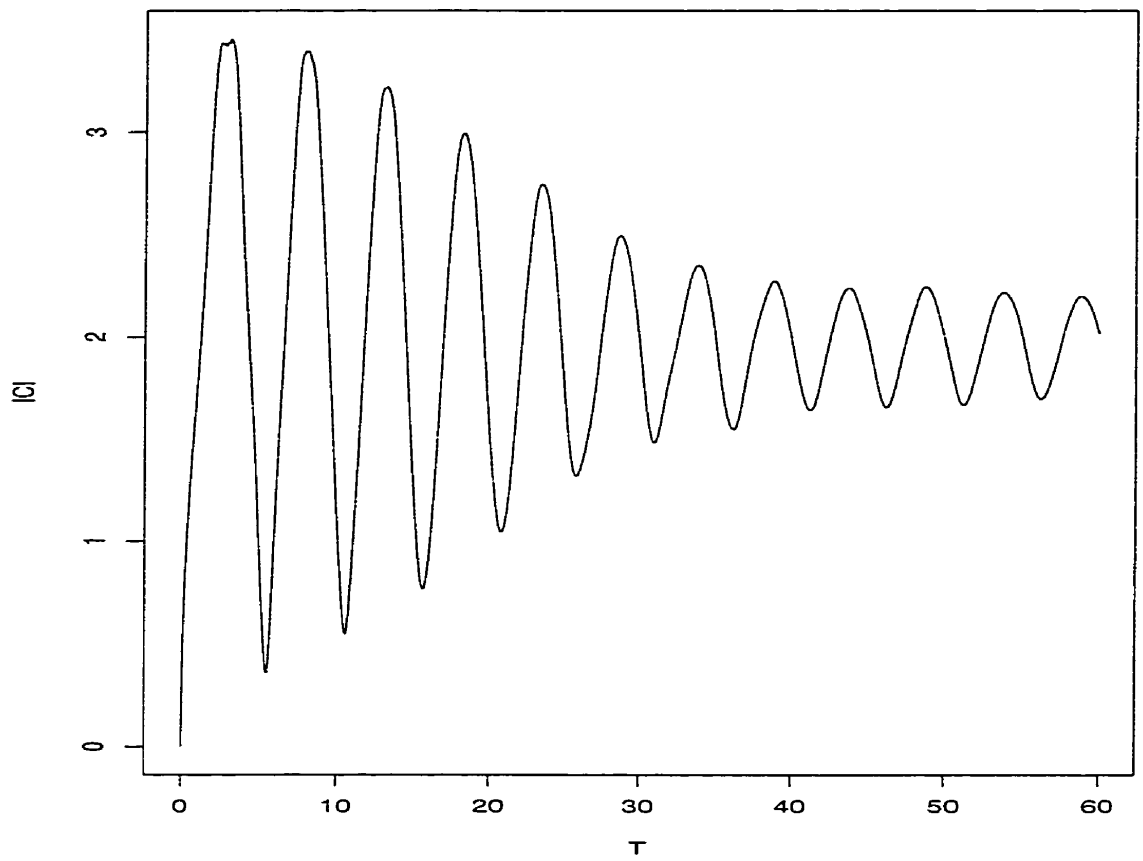

Figure 5.3: Long-term streamfunction behaviour.

for $\lambda = 0.001$. At higher values of λ, the oscillation amplitude does vanish, but to investigate the problem in which viscosity plays a leading-order role in the dynamics is not the objective of this study.) The long-term behaviour of $|C_1|$ is seen in figure (5.3). The rapid amplitude decay is halted near $T = 35$. The behaviour out to $T = 60$ appears to exhibit a very slow decay, but other than that, shows no change out to times at least as long as $T = 100$, so it is believed to be in a quasi-steady state.

5.2 Transient versus Long-time Behaviour

The behaviour of the forced system, therefore, consists of a transient, decaying-amplitude oscillation, followed by a constant amplitude oscillation at long times. The transient behaviour of the vorticity is significantly different from the long-time behaviour. Figure (5.4) is a sequence of snapshots of the vorticity at equally spaced intervals during one of the first oscillation periods (from one maximum in $|C_1|$ to one snapshot shy of the next maximum). Note that the greyscale of each snapshot is set independently so the detail of those plots with smaller maximum amplitudes may be easily seen.

The oscillation is seen to be quite nonlinear in nature, as the flow appears complicated at times. Despite this complexity, one may deduce from figure (5.4) an intuitive explanation for the source of the oscillation. First, note that the forcing acts as a source at $x = 0$ and a sink at $x = \pi$. Secondly, observe that the vortex appears to move to the right in plots (a), (b), and (c) of (5.4). These observations yield the following explanation. The first step in the cycle is that the forcing increases the vorticity near $x = 0$ and decreases it near $x = \pi$. Then the nonlinearity acts to generate coherent vortices at these locations. The nonzero extent of the vortices in the Y direction allows them to be affected by the shear flow which is zero at $Y = 0$ and positive elsewhere, since $U(Y) = Y^2$. This is how the coherent vortices of the unforced problem are transported along the x direction with constant positive speed. However, in the forced problem, when the vortices move, they become out of phase

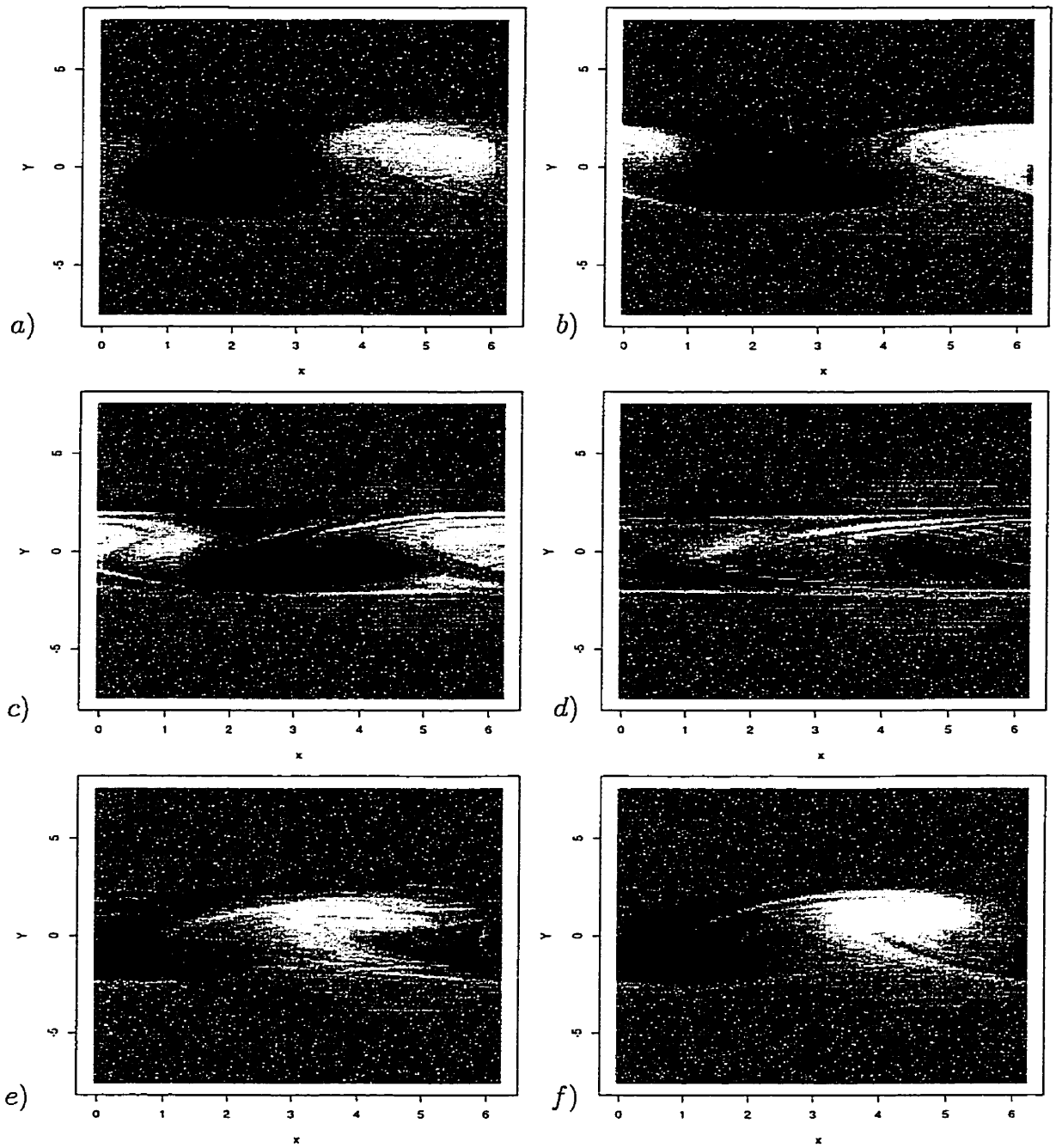

Figure 5.4: Detail of transient vorticity behaviour. Z shown at times (a) 3.2 (max. $|C_1|$), (b) 4.0, (c) 4.8, (d) 5.6 (min. $|C_1|$), (e) 6.4, and (f) 7.2. Greyscale: black=max. value, white=min. value, with maxima of 2.35, 1.66, 1.0, 0.95, 1.35 and 1.87.

with the forcing (this happens in frame (c)). The forcing, which has not moved, then tends to decrease the magnitude of the vortex structures, and effectively destroy them (frame (d)). The entire process then starts again (frames (e) and (f)). Thus, one oscillation essentially consists of vortices being produced by the forcing, swept along one half wavelength by the shear flow, and destroyed again by the forcing.

Given this picture of what is happening at early times, one might expect that the quasi-steady state behaviour at later times would simply be the same behaviour with, perhaps, appropriately diminished amplitudes. However, such is not the case. Figure (5.5) is a series of snapshots showing the behaviour of the vorticity during a typical period of the oscillation when the field is in its quasi-steady state. The behaviour is clearly nothing like that seen for early times. This behaviour appears to be some small departure from the time independent basic state. It is interesting to note that the basic state is one where the vortex structures are $\pi/2$ out of phase with the forcing. This makes sense if one thinks of this final basic state as some sort of balance between the forcing and the advection term.

The nature of the departure from the basic state appears, in figure (5.5), to be a fluctuation in the amplitude of the basic state. To precisely determine the behaviour of the time-dependent part of the vorticity, it was isolated by subtracting the time-averaged vorticity field from the snapshots of figure (5.5). The averaging and subtracting was done over eight frames, and not four as shown in figure (5.5), both to compute a more accurate average and to produce a clearer picture of the motion of

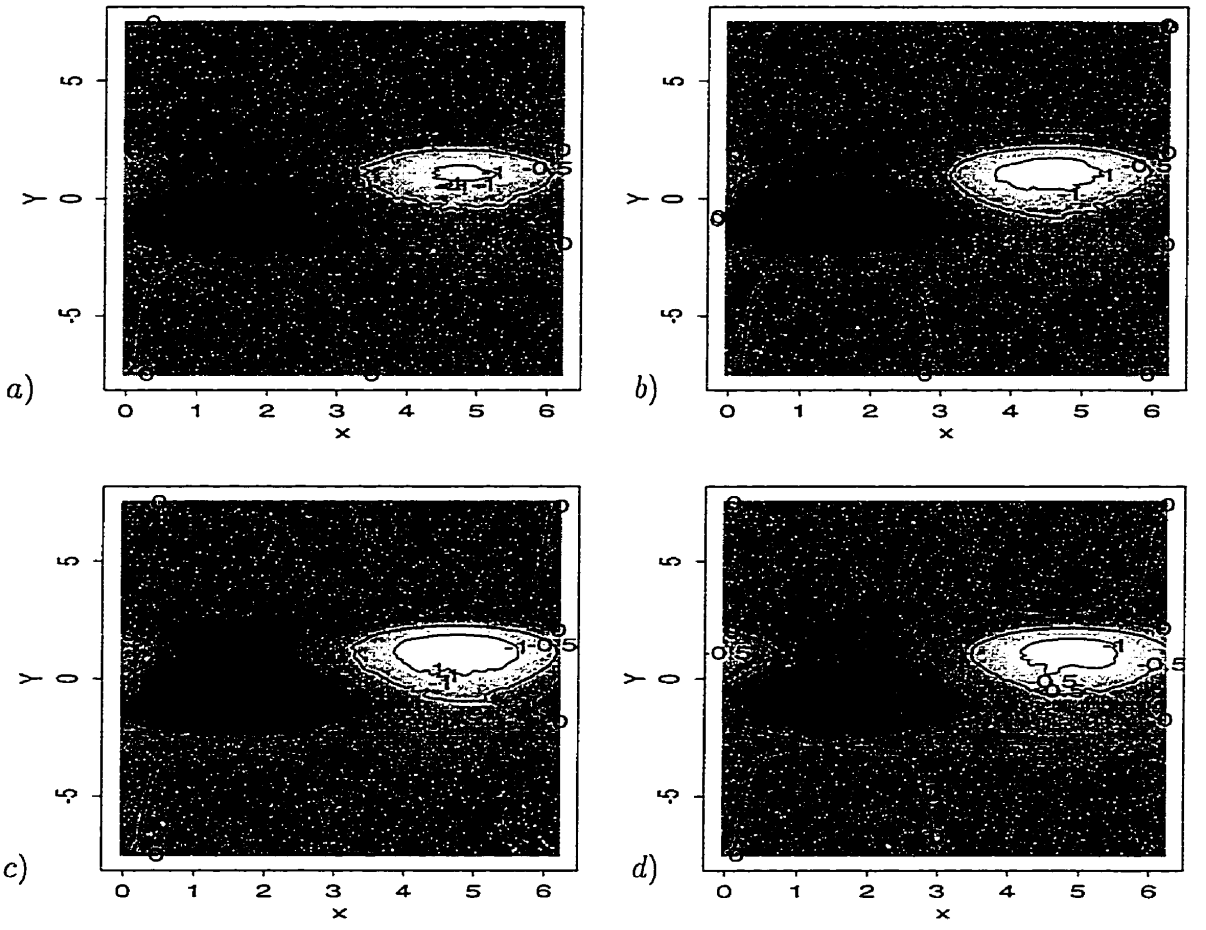

Figure 5.5: Long time vorticity behaviour. Z shown at times (a) 61.4 (min. $|C_1|$), (b) 62.7, (c) 64.0 (max. $|C_1|$), and (d) 65.3. Greyscale: black=1.37, white=-1.37.

the residual vorticity field. The averaging was performed over one period, beginning at $T = 61.4$, by which time the solution has clearly reached its quasi-steady state.

The resulting eight frames are displayed in figures (5.6) and (5.7). The residual time-dependent vorticity appears to be a traveling disturbance with a constant phase speed. Superimposed on this constant phase speed in x is a slight movement in the y direction. As the positive and negative disturbances move to the right, their centres seem to pass slightly below the point $(x, y) = (\pi/2, 0)$ and slightly above the point $(3\pi/2, 0)$. Also seen in these figures is the presence of unphysical gridscale structures: the same averaging process that reveals the behaviour of the residual vorticity makes these gridscale structures conspicuous.

The time variation of $|C_1|$ seen is consistent with this disturbance passing into and out of phase with the time mean vorticity. The speed of the vortex structures is 1.2 in nondimensional units.

Recall that the long-time solution to the unforced problem was in the form of coherent vortex structures traveling in the positive x direction with a constant speed. Does this time-dependent part of the forced solution correspond to the traveling vortices of the unforced problem? The answer seems to be negative, due to several important differences between the two results. First of all, the speed of the vortices in the unforced problem is 1.0, but in the forced problem the speed is 1.2. Secondly, as may be seen from figure (5.1d), the shape of the structures appears qualitatively different. And finally, the unforced case exhibits no motion in the y direction. The

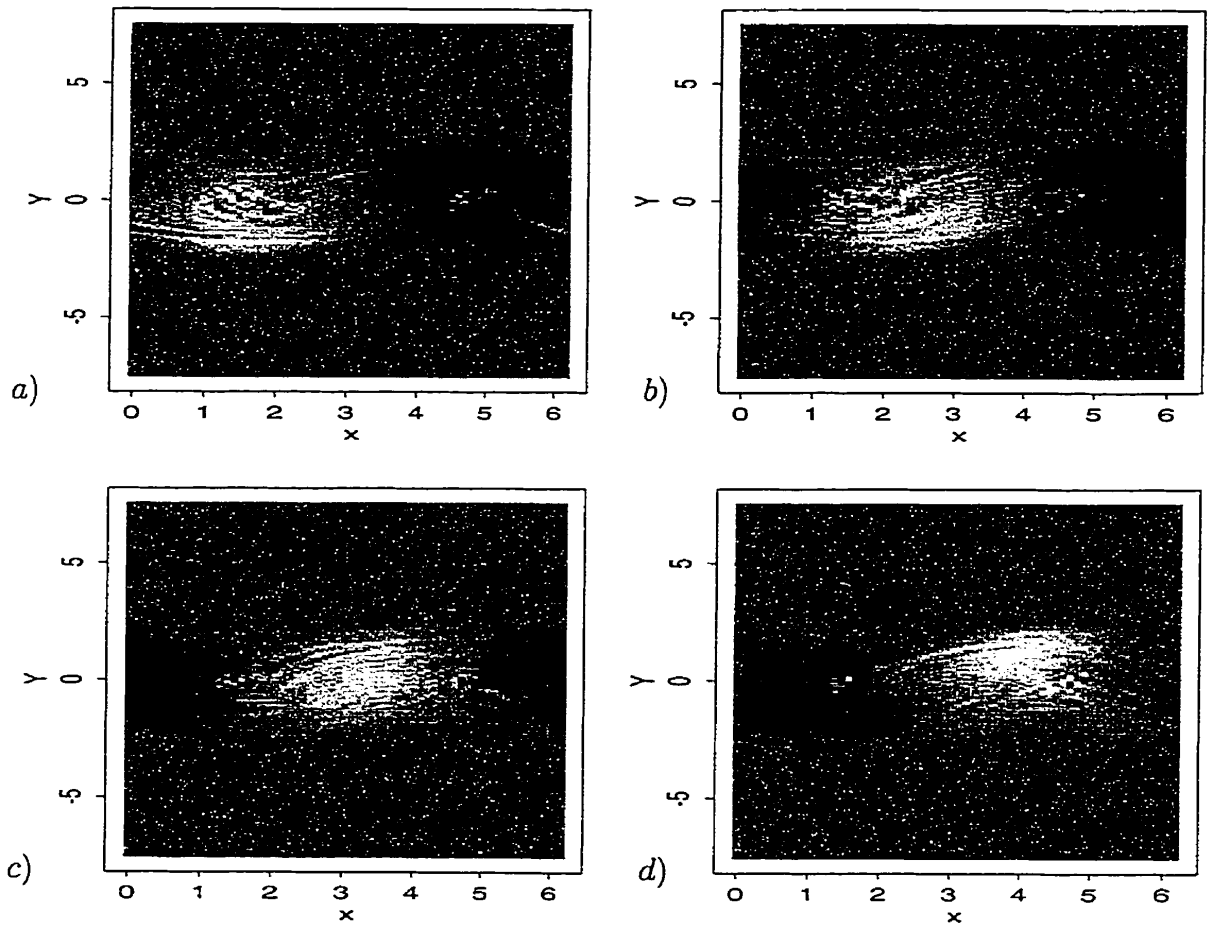

Figure 5.6: Behaviour of time-varying part of vorticity, frames 1–4. $Z - \bar{Z}$ shown at times (a) 61.40 (min. $|C_1|$), (b) 62.05, (c) 62.70, and (d) 63.35.

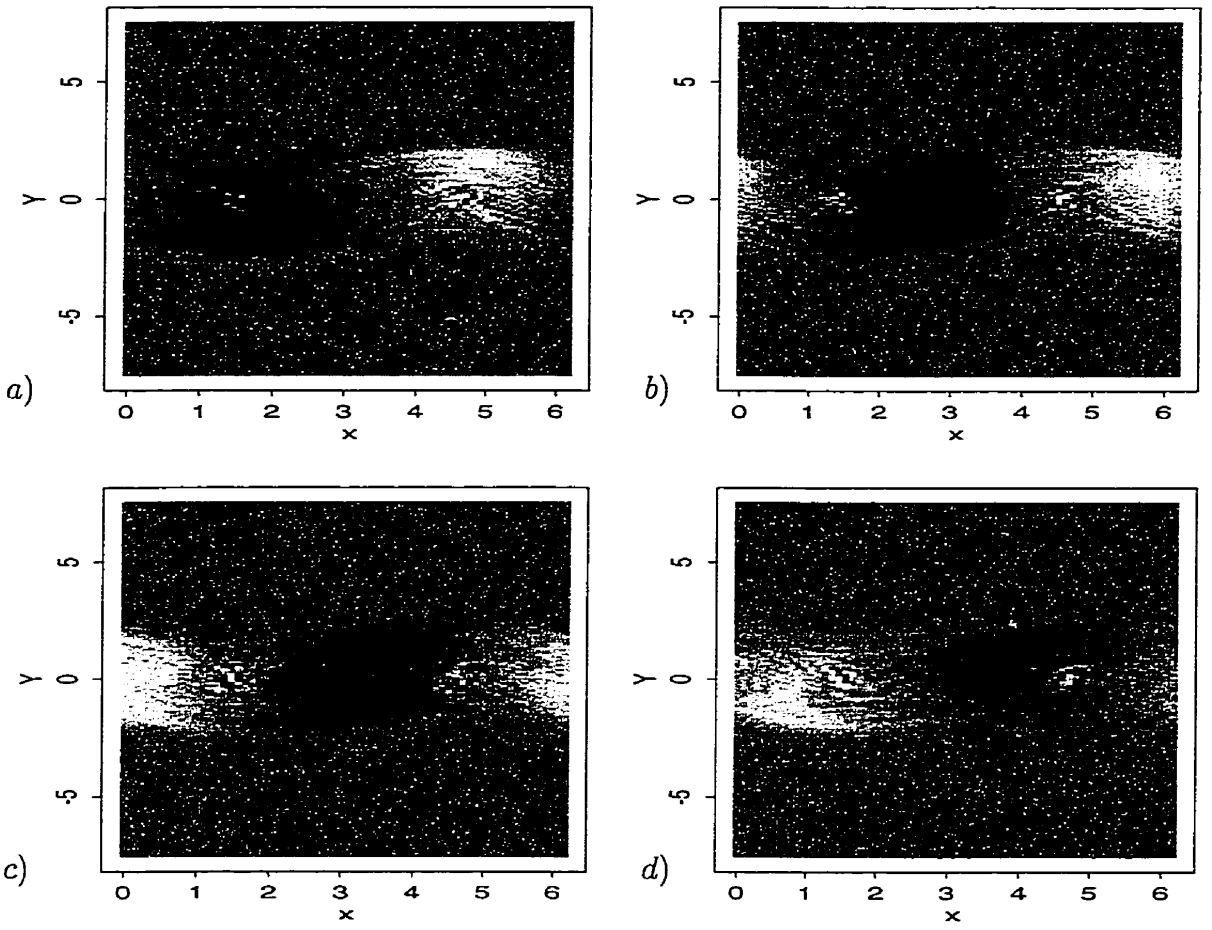

Figure 5.7: Behaviour of time-varying part of vorticity, frames 5–8. $Z - \bar{Z}$ shown at times (a) 64.00 (max. $|C_1|$), (b) 64.65, (c) 65.30, and (d) 65.95.

negative vortices are displaced slightly northward of $y = 0$, and the positive ones slightly southward, but the motion is entirely eastward. The motion in the forced case, however, consists of a small oscillatory motion in the Y direction superimposed upon the constant eastward displacement.

5.3 Analytical Ansatz of Long-time Behaviour

It is not immediately clear how a nonlinear, forced partial differential equation has as its solution a small, steadily traveling disturbance superimposed on a stationary pattern. Given the relatively simple form of the numerical solution at long times, it stands to reason that that form may be reproduced in analytical form. To do so would provide evidence to support the numerical result, and perhaps provide some insight into the solution (such as what determines the phase speed of the traveling part).

The following is an ansatz of the functional form of the vorticity in the critical layer. It does not give a general solution to the equations, but it does show how the terms may balance to produce a traveling wave solution as a perturbation to the stationary part of the vorticity field.

For reference, the governing equation, in nondimensionalized form, in the critical layer is

$$\frac{\partial Z}{\partial T} + Y^2 \frac{\partial Z}{\partial x} + \frac{\partial C}{\partial x}\frac{\partial Z}{\partial Y} = e^{ix} \tag{5.1}$$

with the nth Fourier components of Z and C related by

$$C_n = -\frac{1}{2n}\int_{-\infty}^{\infty} Z_n \, dY. \tag{5.2}$$

Expressing Z (and therefore, C) as the sum of a time independent part plus a time dependent perturbation, we write

$$Z(x,Y,T) = \bar{Z}(x,Y) + Z'(x,Y,T)$$

$$C(x,T) = \bar{C}(x,Y) + C'(x,Y,T).$$

Substituting these forms into equation (5.1), the leading-order equation becomes

$$Y^2\frac{\partial \bar{Z}}{\partial x} + \frac{\partial \bar{C}}{\partial x}\frac{\partial \bar{Z}}{\partial Y} = e^{ix} \tag{5.3}$$

while, at the next order, it is

$$\frac{\partial Z'}{\partial T} + Y^2\frac{\partial Z'}{\partial x} + \frac{\partial C'}{\partial x}\frac{\partial \bar{Z}}{\partial Y} + \frac{\partial \bar{C}}{\partial x}\frac{\partial Z'}{\partial Y} = 0. \tag{5.4}$$

It was observed from the numerical results viewed in phase space that the zeroth and first Fourier modes are much larger in amplitude than higher modes. Also, in a well-defined region near $Y = 0$ (approximately, $|Y| < 2$), the first Fourier mode is observed to be approximately constant in Y, while for larger $|Y|$ (approximately $|Y| > 3$), all modes decay with increasing $|Y|$. The decay for larger $|Y|$ is easily seen in the graphical results of figures (5.2d), and (5.4)–(5.7), and understood by observing that for large Y^2, the terms $Y^2\partial Z/\partial x$ and e^{ix} of equation (5.1) must be in balance. These two regions correspond to the inner and outer regions dealt with in the asymptotic analysis of chapters 2 and 3.

Based on these observations, the following functional form of Z is proposed as an explanation of how a propagating disturbance, which is seen in the region near $Y = 0$, can solve the governing equations:

$$Z = \bar{Z}_0(Y) - i\bar{Z}_1(Y)e^{ix} + iZ_1'(Y,T)e^{ix}$$

$$C = (i/2)e^{ix}\int_{-\infty}^{\infty} \bar{Z}_1(Y)\,dY - (i/2)e^{ix}\int_{-\infty}^{\infty} Z_1'(Y,T)\,dY$$

where $\bar{Z}_0$, $\bar{Z}_1$ and Z_1' are real to leading order. Furthermore, we assume that $\bar{Z}_1$ and Z_1' are constant in Y, and positive. (This only holds in the region near $Y = 0$ discussed above. Indeed, it is the rapid decay in $|Y|$ away from $Y = 0$ that allows the infinite integrals to converge.) The time dependence of Z_1' is left unspecified, since it is the aim of this exercise to show that the above assumptions imply the solution is in the form of a steadily-propagating disturbance.

Instead of seeking the solution to the leading-order equation, we use it to reveal the balance of terms at the next order. Isolating for $\partial\bar{Z}/\partial Y$ gives

$$\frac{\partial\bar{Z}}{\partial Y} = \left(\frac{\partial\bar{C}}{\partial x}\right)^{-1}\left(e^{ix} - Y^2\frac{\partial\bar{Z}}{\partial x}\right). \tag{5.5}$$

Substituting this into the next order equation and utilizing the assumptions gives the following equation:

$$i\frac{\partial Z_1'}{\partial T} - Y^2 Z_1' + \frac{\int_{-\infty}^{\infty} Z_1'\,dY}{\int_{-\infty}^{\infty} \bar{Z}_1\,dY}(-1 + Y^2\bar{Z}_1(Y)) = 0.$$

If the time dependence of Z_1' is e^{-icT}, then we arrive at

$$cZ_1'(Y) - Y^2 Z_1'(Y) + \frac{\int_{-\infty}^{\infty} Z_1'\,dY}{\int_{-\infty}^{\infty} \bar{Z}_1\,dY}(-1 + Y^2\bar{Z}_1(Y)) = 0,$$

where the terms clearly balance in pairs. Denoting $(\int_{-\infty}^{\infty} Z_1' \, dY)/(\int_{-\infty}^{\infty} \bar{Z}_1 \, dY) = \delta$, the equation is solved as long as $Z_1' = \delta \bar{Z}_1$ and $c = \delta / Z_1'$, since both $\bar{Z}_1$ and Z_1' are assumed to be independent of Y in this region. Then Z_1' is indeed a traveling wave solution, with positive phase speed c.

Chapter 6

Conclusions

The motivation for the work of this thesis includes previous analyses of observational data which found that, in the framework of isentropic coordinates, there exist regions in the atmosphere with diminished isentropic potential vorticity (PV) gradients and also regions where heating effects play an important role. Regions where both effects are present are located in the upper troposphere, over the tropical Atlantic and Pacific. The goal of this study, therefore, is to investigate the combined effects of a negligible PV gradient and the presence of heating.

The steps taken to perform this study started with the observation that the two dimensional analogue of PV is absolute vorticity. Next, the profile of the background shear flow was taken to be parabolic in order to eliminate the leading-order absolute vorticity gradient. The barotropic vorticity equation was linearized about this shear flow, and the functional form of the forcing was taken to be sinusoidal in the x

direction, of general form in y, and independent of time.

The solution of the linearized problem shows that the vorticity, in addition to having the sheared nature of the unforced problem, exhibits growth in time, growing the fastest near $y = 0$, as $O(t)$ for $t \gg 1$. The streamfunction grows as $O(t^{1/2})$, and when $t \sim O(\epsilon^{-1/2})$ (where ϵ is the amplitude of the perturbation to the shear flow), a nonlinear critical layer of thickness $O(\epsilon^{1/4})$ is formed about $y = 0$. Within the critical layer, numerical simulations show the growth of the streamfunction is halted, and its magnitude oscillates about a nonzero value. Early in the nonlinear regime, vortex structures are alternately created and destroyed in a complicated fashion, while the streamfunction's oscillation amplitude decays. Ultimately, stationary vortex structures are established (out of phase with the forcing), with smaller-amplitude steadily-propagating vortices superimposed. At this point, the amplitude of the streamfunction oscillates without further decay.

We thus have seen how the effects of the zero absolute vorticity gradient and of the forcing produce an interesting combined effect. While the zero absolute vorticity gradient does not allow waves to propagate in the y direction, the nonlinearity in the critical layer causes the gradient to be locally nonzero, which allows vortex structures to form. The effect of the forcing, in the long term, is to cause these vortex structures to be stationary with respect to the forcing, although $\pi/2$ out of phase with it. In addition, superimposed upon these primary-importance vortices, is a set of smaller-magnitude vortex structures which propagate in the x direction with a constant speed.

There are several extensions to this study which would be interesting to research. The shear flow was chosen for the purpose of setting the absolute vorticity gradient to zero, and not to reflect observed wind behaviour. However, the shape of the shear flow clearly played a direct role in the dynamics seen. A study of the case where the absolute vorticity gradient is made to vanish, if even only locally, by a more physically realistic shear flow, would be interesting.

For example, the Bickley jet, where $U(y) = \mathrm{sech}^2 y$, is a shear flow about which the stability properties are known in detail (Maslowe 1991). The Bickley jet is locally parabolic near the jet maximum at $y = 0$, so the absolute vorticity gradient could be made to vanish there. Therefore, in a problem on the Bickley jet with the same forcing as employed here, it is reasonable to expect the dynamics within a nonlinear critical layer about $y = 0$ to resemble that seen in this work. Additionally, whereas the wind speed for the profile used in this thesis grows to infinity as y moves away from $y = 0$, the Bickley jet wind speed decays to zero in the same limit, which makes the Bickley jet appealing as a realistic model of an isolated wind jet.

Secondly, an extension of this study to three dimensions would be valuable, particularly since PV is, in truth, a three-dimensional quantity, and since it is the vertical variation of heating which generates a PV source. Performing a three-dimensional study could also serve to address the above-mentioned concern of an unrealistic background wind profile. While a more realistic profile in the horizontal direction may be taken, the variation of the shear flow in the vertical direction could be used to nullify

the PV gradient, like Lindzen (1994) has done.

Thirdly, since the choice of the forcing function was an idealized form, there are several improvements in the choice of the forcing that could be made. The traveling forcing studied in Appendix A, which had time dependence in the form $e^{i(kx-\omega t)}$, is more realistic than the steady forcing function. This case was not studied numerically because, as demonstrated in Appendix A, for $\omega = O(1)$, the outer region becomes nonlinear before the critical layer does. However, when $\omega = 0$, as discussed in Chapter 2, it is the critical layer which becomes nonlinear first. This then raises the question of what happens when ω is small but nonzero. If the forcing were made to travel with the same speed as the steadily-traveling vortices of the numerical solution, then one would expect the vortices to grow without bound. Since the vortices travel with speed $O(1)$ in nondimensional critical layer units, and since the nonlinear regime is given by $T = \epsilon^{1/2}t$, this would be expected to occur when $\omega = O(\epsilon^{1/2})$.

Another improvement to the forcing term is motivated by the fact that atmospheric heating, especially over long times, does not closely follow a regular time dependence. Whether or not this time variation of the forcing affects the resulting behaviour could be studied. The effect of the fluctuation could be modeled by expressing the forcing as the sum of a deterministic part plus a random part.

Also, it would be an improvement to study the problem where the forcing term has some dependence upon the vorticity itself, as the governing equations indicate.

Fourthly and finally, the assumption that the forcing and the solution are periodic

in x, and thus extend the entire way around a latitude circle, is clearly a significant simplification. A much more realistic situation would be the one where the forcing, and therefore the solution as well, is localized in x. This would correspond to the wave packet problem where the solution is assumed to be comprised of a narrow spectrum of wavenumbers, instead of merely the one wavenumber.

Appendix A

The Traveling Forcing Problem

A more general problem than the one with stationary forcing is the one with a source that travels at a constant speed with respect to the sheared part of the background flow. That is, suppose the forcing takes the form

$$S(x,y,t) = \sigma(y)e^{i(k(x-U_0t)-\omega t)}. \tag{A.1}$$

Then, carrying out the integration in equation (2.5), the vorticity is found to be

$$\zeta(x,y,t) = \zeta_0\left(x - \tfrac{\beta}{2}y^2t, y\right) + \sigma(y)\frac{\sin\left[t\left(\frac{k\beta}{4}y^2 - \frac{\omega}{2}\right)\right]}{\frac{k\beta}{4}y^2 - \frac{\omega}{2}}e^{ikx}e^{-it\left(\frac{k\beta}{4}y^2+\frac{\omega}{2}\right)}. \tag{A.2}$$

Note that, as in the stationary forcing case, the second term is actually a difference of two complex exponential terms which is written in terms of the sine function to demonstrate plainly that a singularity does not occur where the denominator vanishes.

Also as in the previous case, when $\nabla^2\psi = \zeta$ is inverted to solve for ψ (by assuming the forms $\zeta_0 = \Omega_0(y)e^{ikx}$ and $\psi = e^{ikx}\Phi(y,t)$, and solving for Φ by the method of

Green's functions), the solution splits up neatly into the sum of two terms. We may write

$$\Phi = \Phi_1 + \Phi_2, \tag{A.3}$$

where

$$\Phi_1 = -\frac{1}{2k}\int_{-\infty}^{\infty} e^{-k|y-\xi|}\Omega_0(\xi)e^{-i\frac{k\beta}{2}\xi^2 t}\,d\xi \tag{A.4}$$

is the Brunet and Warn (1990, henceforth BW) result, and

$$\Phi_2 = -\frac{1}{2k}\int_{-\infty}^{\infty} \sigma(\xi)\frac{\sin\left(t(\frac{k\beta}{4}\xi^2 - \frac{\omega}{2})\right)}{\frac{k\beta}{4}\xi^2 - \frac{\omega}{2}} e^{-k|y-\xi|}e^{-it(\frac{k\beta}{4}\xi^2+\frac{\omega}{2})}\,d\xi \tag{A.5}$$

is the result of the forcing.

A.1 The Asymptotic Form for y, $\omega \sim O(1)$

In determining the long-time asymptotic nature of Φ_2, the first step is to rewrite the integrand to eliminate the absolute value signs,

$$\begin{aligned}\Phi_2 \;=\; -\frac{1}{2k}\Bigg[&\int_{-\infty}^{y} \sigma(\xi)\frac{\sin\left(t(\frac{k\beta}{4}\xi^2 - \frac{\omega}{2})\right)}{\frac{k\beta}{4}\xi^2 - \frac{\omega}{2}} e^{-k(y-\xi)}e^{-it(\frac{k\beta}{4}\xi^2+\frac{\omega}{2})}\,d\xi \\ &+ \int_{y}^{\infty} \sigma(\xi)\frac{\sin\left(t(\frac{k\beta}{4}\xi^2 - \frac{\omega}{2})\right)}{\frac{k\beta}{4}\xi^2 - \frac{\omega}{2}} e^{-k(\xi-y)}e^{-it(\frac{k\beta}{4}\xi^2+\frac{\omega}{2})}\,d\xi\Bigg].\end{aligned} \tag{A.6}$$

Now consider these integrands to be functions of a complex variable (z, say, where ξ is the real part of z). Then the above integration is actually performed in the complex plane, with the contour being a straight line segment along the real axis. Since each integrand is clearly analytic everywhere, the contour may be deformed arbitrarily without changing the value of the integral. Therefore, a contour is chosen such that

the points in the plane which make the denominators in the integrals vanish are avoided. Let us these points be denoted by $\pm z_0$. Such a contour is shown in figure A.1. On C, the denominators of the integrands are never zero, so it is convenient to rewrite the integral by expressing $\sin x$ as the difference of two complex exponentials, and to integrate over each resulting term separately. The result is

$$\begin{aligned}\Phi_2 \;=\; -\frac{1}{2k}\Bigg[&\int_{C:-\infty}^{y}\sigma(z)\frac{e^{-i\omega t}}{i(\frac{k\beta}{2}z^2-\omega)}e^{-k(y-z)}\,dz\\ &-\int_{C:-\infty}^{y}\sigma(z)\frac{e^{-i\frac{k\beta}{2}z^2 t}}{i(\frac{k\beta}{2}z^2-\omega)}e^{-k(y-z)}\,dz\\ &+\int_{C:y}^{\infty}\sigma(z)\frac{e^{-i\omega t}}{i(\frac{k\beta}{2}z^2-\omega)}e^{-k(z-y)}\,dz\\ &-\int_{C:y}^{\infty}\sigma(z)\frac{e^{-i\frac{k\beta}{2}z^2 t}}{i(\frac{k\beta}{2}z^2-\omega)}e^{-k(z-y)}\,dz\Bigg],\end{aligned} \tag{A.7}$$

where the limits denote that the integrals are to be evaluated along the contour C, between the displayed limits. This expression is not valid for the special cases $y = z_0$ or $y = -z_0$ (since $z = y$ would not be on C), so these cases will be treated separately later.

Now, each of the integrals along C will have a contribution from the Cauchy prin-

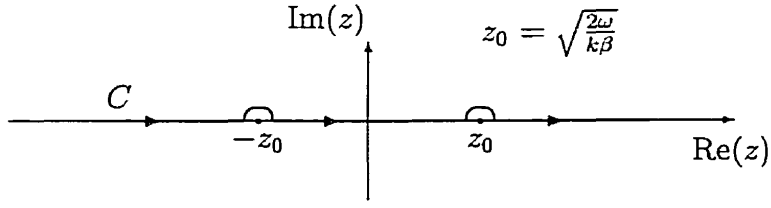

Figure A.1: The deformed contour C in the complex plane

cipal value of the integral along the real axis and a contribution from one, both, or neither (depending on the value of y) of the deformations about $\pm z_0$. The contribution from each deformation to the integral it belongs to is $-i\pi \mathrm{Res}(\pm z_0)$. Since $e^{-i\omega t} = e^{-i\frac{k\beta}{2}z_0^2 t}$ (by the definition of z_0), the residue contribution to the first integral will exactly cancel with the residue contribution to the second integral. The same cancellation occurs between the third and fourth integrals. Thus, only the Cauchy principal values of the integrals over the real variable ξ remain,

$$\begin{aligned}
\Phi_2 \;=\; -\frac{1}{2ki}\Bigg[& e^{-i\omega t}\mathcal{P}\int_{-\infty}^{y}\sigma(\xi)\frac{1}{\frac{k\beta}{2}\xi^2-\omega}e^{-k(y-\xi)}\,d\xi \\
& - \quad \mathcal{P}\int_{-\infty}^{y}\sigma(\xi)\frac{e^{-i\frac{k\beta}{2}\xi^2 t}}{\frac{k\beta}{2}\xi^2-\omega}e^{-k(y-\xi)}\,d\xi \\
& + \; e^{-i\omega t}\mathcal{P}\int_{y}^{\infty}\sigma(\xi)\frac{1}{\frac{k\beta}{2}\xi^2-\omega}e^{-k(\xi-y)}\,d\xi \\
& - \quad \mathcal{P}\int_{y}^{\infty}\sigma(\xi)\frac{e^{-i\frac{k\beta}{2}\xi^2 t}}{\frac{k\beta}{2}\xi^2-\omega}e^{-k(\xi-y)}\,d\xi\Bigg]. \qquad \text{(A.8)}
\end{aligned}$$

The long time asymptotic behaviour of Φ_2 may now be deduced from the above form. The first and third terms clearly oscillate in time with a constant amplitude. The second and fourth integrals, however, each have a rapidly oscillating integrand which causes the integrals to decay with time.

To calculate the decay rate, the method of stationary phase is used. The stationary phase point in each integral is $\xi = 0$, so only one of the two integrals will contain that point, depending on whether $y > 0$ or $y < 0$. The other integral will decay with an even faster rate, its main contribution coming from the vicinity of the (finite) endpoint of the interval integrated over. Assuming first that $y > 0$, so that the second

integral contains the stationary phase point, it is found that

$$-\mathcal{P}\int_{-\infty}^{y}\sigma(\xi)\frac{e^{-i\frac{k\beta}{2}\xi^2 t}}{\frac{k\beta}{2}\xi^2-\omega}e^{-k(y-\xi)}\,d\xi \sim \sigma(0)\frac{e^{-i\pi/4}}{\omega}e^{-ky}\left(\frac{2\pi}{k\beta t}\right)^{1/2}+O(t^{-1}). \qquad (A.9)$$

If $y<0$, the fourth integral in (A.8) will contain the stationary phase point. The only difference in the result is that e^{-ky} becomes e^{ky}. So the above asymptotic expression is still valid, as long as the result is expressed in terms of the absolute value of y. For small y (to be precise, when $\frac{k\beta}{2}y^2t \sim O(1)$), the stationary phase point will make some contribution to each of the second and fourth integrals. A separate analysis will be done to determine the asymptotic behaviour in that case (see The Inner Region Asymptotic Behaviour below).

The asymptotic form of Φ_2 may now be written. For brevity, the first and third integrals in (A.8) are combined into one term and denoted as

$$F(y,\omega)=\mathcal{P}\int_{-\infty}^{\infty}\sigma(\xi)\frac{1}{\frac{k\beta}{2}\xi^2-\omega}e^{-k|y-\xi|}\,d\xi, \qquad (A.10)$$

so that the result may be written

$$\Phi_2 \sim -\frac{1}{2ki}e^{-i\omega t}F(y,\omega)-\frac{\sigma(0)e^{-i\pi/4}}{i\omega k}e^{-k|y|}\left(\frac{\pi}{2k\beta t}\right)^{\frac{1}{2}}+O(t^{-1}). \qquad (A.11)$$

Recalling the BW result,

$$\Phi_1 \sim -\Omega_0(0)\frac{e^{-i\pi/4}}{k}e^{-k|y|}\left(\frac{\pi}{2k\beta t}\right)^{\frac{1}{2}}+O(t^{-1}), \qquad (A.12)$$

the asymptotic for the streamfunction may finally be written

$$\begin{aligned}\psi \sim e^{ikx}\Big[&-\frac{1}{2ki}e^{-i\omega t}F(y,\omega)\\ &-\left(\frac{\sigma(0)}{i\omega}+\Omega_0(0)\right)\frac{e^{-i\pi/4}}{k}e^{-k|y|}\left(\frac{\pi}{2k\beta t}\right)^{\frac{1}{2}}+O(t^{-1})\Big]. \qquad (A.13)\end{aligned}$$

It has been already noted that the argument used in the derivation of the above expression is not valid for the special cases $y = \pm z_0$ (where the denominator of the integrand vanishes). However, it turns out that the asymptotic expression found (i.e. equation (A.13)) is valid even when $y = \pm z_0$. This can be understood by noting first that the integrand in (A.5) is not singular, even when $\xi = \pm z_0$. Secondly, we see that y is not *really* an endpoint of the integrals, it is merely where the expression within the absolute value brackets changes sign. The validity of equation (A.13) when $y = z_0$, say, can be proven rigorously by expressing the integrals in equation (A.6) as the sum of the Cauchy principal value integrals in equation (A.8) plus an integral over the interval $(z_0 - \epsilon, z_0)$ of the first integrand in (A.6) plus an integral over the interval $(z_0, z_0 + \epsilon)$ of the second integrand in (A.6). Since the integrands are continuous, in the limit as $\epsilon \to 0$, the latter two contributions vanish, leaving the Cauchy principal value integral contributions. Thus we will arrive at the same result.

Using the above form, the timescale at which the nonlinear terms in the governing equation grow to leading-order importance may be determined. Recall that the vorticity is given by equation (A.2). It is found that

$$\begin{array}{ccccccccc} \zeta_t & + & \frac{\beta}{2} y^2 \zeta_x & + & \epsilon(\psi_x \zeta_y & - & \psi_y \zeta_x) & = & \sigma(y) e^{ikx} \\ O(1) & & O(1)O(1) & & \epsilon O(1)O(t) & & \epsilon O(1)O(1) & & O(1), \end{array}$$

and therefore the nonlinear terms become important (in the region $y \sim O(1)$, and when $\omega \sim O(1)$) when $t \sim O(\epsilon^{-1})$.

A.2 The Inner Region Asymptotic Behaviour

The inner region is investigated by letting $\eta = (k\beta t/2)^{1/2} y = O(1)$. Also, we denote equation (A.3) as

$$\Phi(\eta, t) = \tilde{\Phi}_1(\eta, t) + e^{-i\omega t}\tilde{F}(\eta, t) + \tilde{\Phi}_2(\eta, t), \tag{A.14}$$

so that $\tilde{\Phi}_1$ is the BW solution in the critical layer, $\tilde{F}$ is the combination of the first and third integrals in equation (A.8), and $\tilde{\Phi}_2$ is the combination of the second and fourth integrals in equation (A.8). Notice that, since $F(y, \omega)$ of the previous section is valid for all y, we simply have $\tilde{F}(\eta, t) = F(\sqrt{2/(k\beta t)}\eta, \omega)$. We recall here the BW result,

$$\tilde{\Phi}_1 \sim \left[-\left(\frac{\pi}{2k\beta t}\right)^{1/2}\frac{e^{-i\pi/4}}{k} + \frac{2\eta}{k\beta t}\int_0^\eta e^{-is^2}\,ds\right]\Omega_0(0) + O(t^{-3/2}). \tag{A.15}$$

Now, if the change of variables $s = (k\beta t/2)^{1/2}\xi$ is made in the second and fourth integrals of equation (A.8), then

$$\begin{aligned}\tilde{\Phi}_2 \;=\; & -\frac{1}{ki}\left(\frac{1}{2k\beta t}\right)^{1/2}\left[\mathcal{P}\int_{-\infty}^{\eta}\sigma\left(\sqrt{\tfrac{2}{k\beta t}}s\right)\frac{e^{-is^2}}{\frac{s^2}{t}-\omega}e^{-(\frac{2k}{\beta t})^{1/2}(\eta - s)}\,ds\right. \\ & \left. +\mathcal{P}\int_{\eta}^{\infty}\sigma\left(\sqrt{\tfrac{2}{k\beta t}}s\right)\frac{e^{-is^2}}{\frac{s^2}{t}-\omega}e^{-(\frac{2k}{\beta t})^{1/2}(s - \eta)}\,ds\right].\end{aligned} \tag{A.16}$$

The approximations $\sigma((k\beta t)^{-1/2}s) \approx \sigma(0)$ and $\frac{s^2}{t} - \omega \approx -\omega$ are employed since terms smaller than $O(t^{-1/2})$ within the square brackets will be neglected (and since, by assumption, $\sigma(y)$ is a slowly varying function). Then $\tilde{\Phi}_2$ may be re-written as

$$\begin{aligned}\tilde{\Phi}_2 \;=\; & -\frac{\sigma(0)}{i\omega k}\left(\frac{2}{k\beta t}\right)^{1/2}\left[\cosh\left(\left(\tfrac{2k}{\beta t}\right)^{\frac{1}{2}}\eta\right)\int_0^\infty e^{-(\frac{2k}{\beta t})^{1/2}s}e^{-is^2}\,ds\right. \\ & \left. -\int_0^\eta \sinh\left(\left(\tfrac{2k}{\beta t}\right)^{\frac{1}{2}}(\eta - s)\right)e^{-is^2}\,ds\right].\end{aligned} \tag{A.17}$$

Finally, by expanding in powers of t, the following result is found:

$$\tilde{\Phi}_2 \sim \left[-\left(\frac{\pi}{2k\beta t}\right)^{1/2}\frac{e^{-i\pi/4}}{k} + \frac{2}{k\beta t}\left(-\frac{i}{2}e^{-i\eta^2} + \eta\int_0^\eta e^{-is^2}\,ds\right)\right]\frac{\sigma(0)}{i\omega} + O(t^{-3/2}). \quad \text{(A.18)}$$

Thus, the asymptotic forms of ψ ($\psi = e^{ikx}\Phi(\eta, t)$, where Φ is as given in (A.14)) and ζ (which is still given by (A.2)) are known. Substituting these forms into the vorticity equation to determine when the nonlinear terms become of leading-order importance,

$$\begin{array}{ccccccccc} \zeta_t & + & \frac{\beta}{2}y^2\zeta_x & + & \epsilon(\psi_x\zeta_y & - & \psi_y\zeta_x) & = & \sigma(y)e^{ikx} \\ O(1) & & O(t^{-1})O(1) & & \epsilon O(1)O(t^{1/2}) & & \epsilon O(t^{-1/2})O(1) & & O(1) \end{array}$$

so the nonlinear terms become important near $y = O(t^{-1/2})$ at $t \sim O(\epsilon^{-2})$. When $y = O(1)$, the nonlinear terms become important at $t \sim O(\epsilon^{-1})$, *before* the inner region becomes nonlinear. Since the solution becomes nonlinear first in the outer region, a numerical study of the nonlinear solution was not pursued.

Bibliography

[1] Brown, S. N., and K. Stewartson, 1980: On the algebraic decay of disturbances in a stratified shear flow. *J. Fluid Mech.*, **100**, 811–816.

[2] Brunet, G., and T. Warn, 1990: Rossby wave critical layers on a jet. *J. Atmos. Sci.*, **47**, 1173–1178.

[3] Brunet, G., and P. H. Haynes, 1995: The nonlinear evolution of disturbances to a parabolic jet. *J. Atmos. Sci.*, **52**, 464–477.

[4] Brunet, G., and P. H. Haynes, 1996: Low-latitude reflection of Rossby wave trains. *J. Atmos. Sci.*, **53**, 482–496.

[5] Brunet, G., R. Vautard, B. Legras, and S. Edouard, 1995: Potential vorticity on isentropic surfaces: climatology and diagnostics. *Mon. Wea. Rev.*, **123**, 1037–1058.

[6] Edouard, S., R. Vautard, and G. Brunet, 1997: On the maintenance of potential vorticity in isentropic coordinates. *Quart. J. Roy. Meteor. Soc.*, in press.

[7] Grotjahn, R., 1993: *Global Atmospheric Circulations: Observations and Theories*, Oxford University Press, 430 pp.

[8] Haynes, P. H., 1989: The effect of barotropic instability on the nonlinear evolution of a Rossby wave critical layer. *J. Fluid Mech.*, **207**, 231–266.

[9] Haynes, P. H., and M. E. McIntyre, 1987: On the evolution of vorticity and potential vorticity in the presence of diabatic heating and frictional or other forces. *J. Atmos. Sci.*, **44**, 828–841.

[10] Hoerling, M. P., 1992: Diabatic sources of potential vorticity in the general circulation. *J. Atmos. Sci.*, **49**, 2282–2292.

[11] Holton, J. R., 1992: *An Introduction to Dynamic Meteorology*, 3rd ed. Academic Press, 507 pp.

[12] Hoskins, B. J., 1991: Towards a PV–θ view of the general circulation. *Tellus*, **43AB**, 27–35.

[13] Hoskins, B. J., M. E. McIntyre, and A. W. Robertson, 1985: On the use and significance of isentropic potential vorticity maps. *Quart. J. Roy. Meteor. Soc.*, **111**, 877–946.

[14] Juckes, M. N., and M. E. McIntyre 1987: A high-resolution one-layer model of breaking planetary waves in the stratosphere. *Nature*, **328**, 590–596.

[15] Killworth, P. D., and M. E. McIntyre, 1985: Do Rossby-wave critical layers absorb, reflect or overreflect? *J. Fluid Mech.*, **161,** 449–492.

[16] Lindzen, R. S., 1994: The Eady problem for a basic state with zero PV gradient but $\beta \neq 0$. *J. Atmos. Sci.*, **51,** 3221–3226.

[17] Maslowe, S. A., 1991: Barotropic instability of the Bickley jet. *J. Fluid Mech.*, **229,** 417–426.

[18] Maslowe, S. A., 1986: Critical layers in shear flows. *Ann. Rev. Fluid Mech.*, **18,** 405–432.

[19] Maslowe, S. A., and L. G. Redekopp, 1979: Solitary waves in shear flows. *Geophys. Astrophys. Fluid Dynamics,* **13,** 185–196.

[20] Press, W. H., S. A. Teukolsky, W. T. Vetterling, and B. P. Flannery, 1992: *Numerical Recipes in FORTRAN*, 2nd ed. Cambridge University Press, 963 pp.

[21] Ritchie, H., 1985: Rossby wave resonance in the presence of a nonlinear critical layer. *Geophys. Astrophys. Fluid Dynamics,* **31,** 49–92.

[22] Sneddon, I., 1972: *The Use of Integral Transforms.* McGraw-Hill, 539 pp.

[23] Stewartson, K., 1978: The evolution of the critical layer of a Rossby wave. *Geophys. Astrophys. Fluid Dynamics,* **9,** 185–200.

[24] Tung, K. K., 1983: Initial-value problems for Rossby waves in a shear flow with a critical level. *J. Fluid Mech.*, **133,** 443–469.

[25] Warn, T, and H. Warn, 1978: The evolution of a nonlinear critical level. *Stud. Appl. Math.*, **59**, 37–71.

IMAGE EVALUATION
TEST TARGET (QA-3)

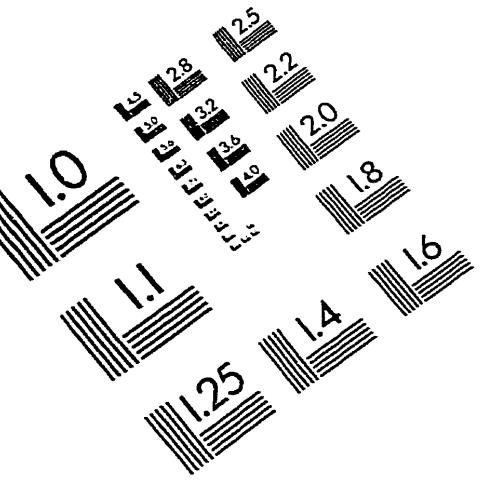

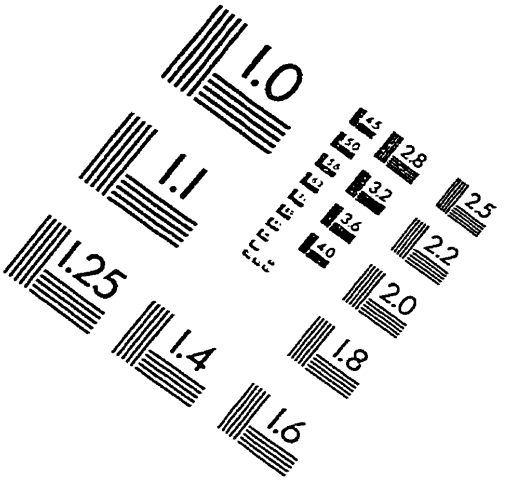

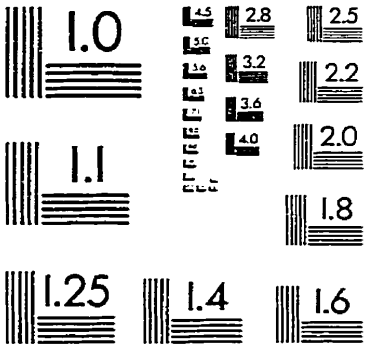

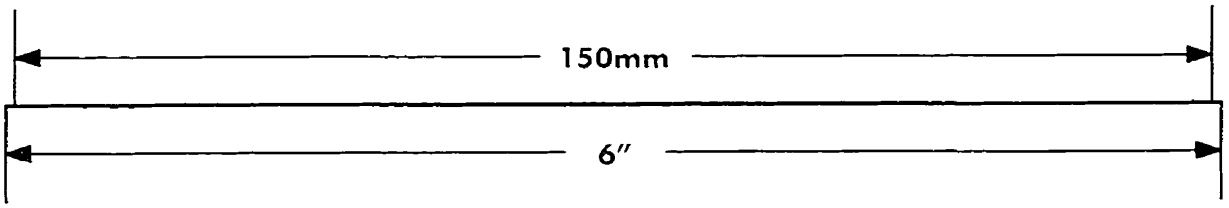

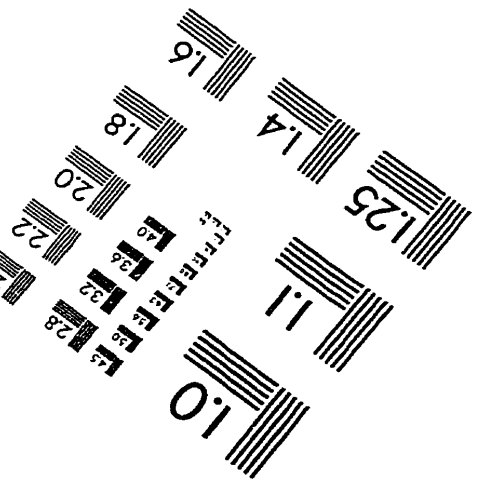

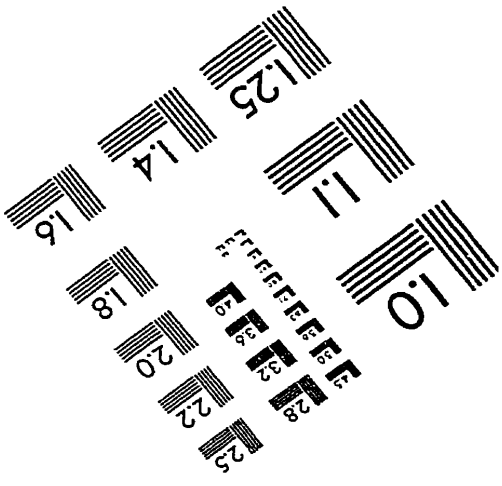

APPLIED IMAGE, Inc
1653 East Main Street
Rochester, NY 14609 USA
Phone: 716/482-0300
Fax: 716/288-5989